

1

2 **Anthropogenic VOC in Abidjan, southern West Africa: from source** 3 **quantification to atmospheric impacts**

4

5 Pamela Dominutti^{1*}, Sekou Keita ^{2,3}, Julien Bahino^{2,3}, Aurélie Colomb¹, Cathy Liousse², Veronique
6 Yoboué³, Corinne Galy-Lacaux², Eleanor Morris⁴, Laëtitia Bouvier¹, Stéphane Sauvage⁵ and Agnès
7 Borbon¹

8

9 ¹ Université Clermont Auvergne, CNRS, Laboratoire de Météorologie Physique (LaMP), F-63000 Clermont-Ferrand,
10 France.

11 ² Laboratoire d'Aérodologie, Université Paul Sabatier Toulouse 3 - CNRS, Toulouse, France

12 ³ Laboratoire de Physique de l'Atmosphère (LAPA)- Université Felix Houphouët-Boigny, Abidjan, Côte d'Ivoire

13 ⁴ Wolfson Atmospheric Chemistry Laboratories, Department of Chemistry, University of York, Heslington, York,
14 YO10 5DD, UK

15 ⁵ IMT Lille Douai, Sciences de l'Atmosphère et Génie de l'Environnement (SAGE), Douai, France

16 **Now at Wolfson Atmospheric Chemistry Laboratories, Department of Chemistry, University of York, Heslington,*
17 *York, YO10 5DD, UK*

18

19 Correspondence to P. Dominutti (pamela.dominutti@york.ac.uk) + A. Borbon (agnes.borbon@uca.fr)

20

21 **Abstract**

22 Several field campaigns were conducted in the framework of the Dynamics-Aerosol-Chemistry-Cloud Interactions
23 in West Africa (DACCIWA) project to measure a broad range of atmospheric constituents. Here we present the
24 analysis of an unprecedented and comprehensive dataset integrating up to fifty-six volatile organic compounds
25 (VOCs) from ambient sites and emission sources. VOCs were collected on multisorbent tubes in the coastal city of
26 Abidjan, Côte d'Ivoire, in winter and summer 2016 and later analysed by gas chromatography coupled with flame
27 ionization and mass spectrometer detectors (GC-FID and GC-MS) at the laboratory.

28 The comparison between VOC emission source profiles and ambient profiles suggests the substantial impact of two-
29 stroke motorized two-wheel vehicles and domestic fires on the composition of Abidjan's atmosphere. However,
30 despite high VOC concentrations near-source, moderate ambient levels were observed (by a factor of 10 to 4000
31 lower), similar to the concentrations observed in northern mid-latitude urban areas. Besides photochemistry, the
32 reported high wind speeds seem to be an essential factor that regulates air pollution levels in Abidjan.

33 Emission ratios ($\Delta\text{VOC}/\Delta\text{CO}$) were established based on real-world measurements achieved for a selected number
34 of representative combustion sources. Maximum measured molar mass emissions were observed from two-wheel
35 vehicles, surpassing other regional sources by two orders of magnitude. Local practices like waste burning also make
36 a significant contribution to VOC emissions, higher than those from light-duty vehicles by 1.5 to 8 orders of
37 magnitude. These sources also largely govern the VOC's atmospheric impacts in terms of OH reactivity, secondary

38 organic aerosol formation (SOAP) and photochemical ozone creation potential (POCP). While the contribution of
39 aromatics dominates the atmospheric impact, our measurements reveal the systematic presence of anthropogenic
40 terpenoids in all residential combustion sectors. Finally, emission factors were used to retrieve and quantify VOC
41 emissions from the main anthropogenic source sectors at the national level. Our detailed estimation of VOC emissions
42 suggests that the road transport sector is the dominant source in Côte d'Ivoire, emitting around 1200 Gg yr⁻¹ of gas-
43 phase VOCs. These new estimates are 100 and 160 times larger than global inventory estimations from MACCity or
44 EDGAR (v4.3.2), respectively. Additionally, the residential sector is largely underestimated in the global emission
45 inventories, by a factor of 13 to 43. Considering only Côte d'Ivoire, these new estimates for VOCs are three to six
46 times higher than the whole of Europe. Given the significant underestimation of VOC emissions from transport and
47 residential sectors in Côte d'Ivoire, there is an urgent need to build more realistic and region-specific emission
48 inventories for the entire West African region. This might be not only true for VOCs but for all atmospheric
49 pollutants. The lack of waste burning, wood fuel burning and charcoal burning and fabrication representation in
50 regional inventories also needs to be addressed, particularly in low-income areas where these types of activities are
51 ubiquitous sources of VOC emissions.

52

53 **Keywords: VOCs, emission inventories, West Africa, air pollution, emission ratios.**

54

55 **1. Introduction**

56 The West Africa region, located to the north of the Gulf of Guinea, is one of the most populated areas in Africa with
57 more than 300 million inhabitants in 2016 (United Nations, 2017). The population has increased by a factor of five
58 since 1950, making West Africa the fastest growing region in the world. Furthermore, future projections indicate
59 population densities in developing countries will continue to increase. The impact in Africa will be particularly high,
60 with projections indicating that the population of the continent could represent 40% of the world's population by
61 2100 (United Nations, 2017). The unplanned explosive growth of urban centres in the region is a significant issue,
62 with water access, air pollution, health problems and unregulated emissions being identified as major concerns.

63 These emissions can produce diverse effects on atmospheric chemistry which are enhanced by severe photochemical
64 conditions and dynamic atmospheric interactions. The atmospheric composition over West Africa is affected by air
65 masses transported from remote sources, i.e., aerosol dust from the Sahara Desert, biomass burning plumes and local
66 urban pollution (Knippertz et al., 2017; Mari et al., 2011). Observations performed during the AMMA (African
67 Monsoon Multidisciplinary Analysis, West Africa, 2005-2006) campaign showed that air quality issues are
68 predominantly related to traffic and combustion emissions (Mari et al., 2011). Residential emissions in southern West
69 Africa (SWA) are attributed to charcoal and wood burning as they are primary sources of domestic energy, widely
70 used for cooking and heating activities. Regional biomass burning is a significant source of carbonaceous aerosols
71 and volatile organic compounds (VOCs) that can have effects on public health and climate through the formation of
72 secondary pollutants (Gilman et al., 2015; Knippertz et al., 2015b; Sommers et al., 2014).

73 Additionally, in most of the southern West Africa cities, traffic emissions are major sources of air pollution (Assamoi
74 and Liousse, 2010). The road transport sector is largely disorganized due to the underdevelopment of road networks
75 and to the absence of a regulation policy for public transportation (Assamoi and Liousse, 2010). As a result, two-
76 wheel vehicles are widely used in the cities for short-distance travel, replacing public transport. Furthermore, the

77 vehicle fleet has increased in the last year, which is characterized in most cities by a large number of old vehicles
78 (Keita et al., 2018). Over the next few years, African emissions from the combustion of fossil fuels, biofuels, and
79 refuse are expected to increase considerably and could represent about 50% of the global emissions of organic carbon
80 (Knippertz et al., 2017; Lioussé et al., 2014). However, emission estimates are uncertain and detailed emission
81 inventories are still required for a better estimation of their impacts on climate change and health over this highly
82 sensitive region (Knippertz et al., 2017).

83 VOCs include a large number of species which can affect air quality by producing secondary pollutants such as ozone
84 and secondary organic aerosols (Seinfeld and Pandis, 2006). Given the reactive nature of VOCs (Atkinson and Arey,
85 2003), VOC emissions need to be disaggregated by species or species groups for a better representation of their
86 chemical features, and to assess their impacts on the secondary formation processes. As VOCs are significant
87 pollutants present in urban atmospheres, in-situ VOC observations are necessary to directly assess exposure and to
88 improve the prediction of secondary product formation.

89 Several field campaigns have been conducted in the last twenty years all over the world with the purpose of
90 characterizing VOC species to better understand their emission sources and fate (Bechara et al., 2010; Bon et al.,
91 2011; Borbon et al., 2013; Brito et al., 2015; Dominutti et al., 2016; Kumar et al., 2018; Salameh et al., 2015; Wang
92 et al., 2014; Warneke et al., 2007). In particular, VOC field observations have been intensely used as constraints for
93 the development of reliable emission inventories (Borbon et al., 2013; Boynard et al., 2014; Gaimoz et al., 2011;
94 Niedojadlo et al., 2007; Salameh et al., 2016b). Some of these studies pointed out significant discrepancies between
95 inventory estimations and emission ratios derived from ambient measurements, implying some limitations in the
96 accurate modelling of VOCs impacts. For northern mid-latitude cities, discrepancies up to a factor of 10 for VOC
97 emissions have been observed (Borbon et al., 2013; Boynard et al., 2014). Such discrepancies are expected to be even
98 more substantial in places of the developing world with high anthropogenic pressures like Africa and South America
99 (Huang et al., 2017). For Africa in particular, the emission inventories frequently used are those developed for global
100 scales due to the lack of observations, which involve numerous uncertainties (Keita et al., 2018; Lioussé et al., 2014).
101 While global emission inventories commonly estimate the total mass of speciated VOCs, they fail in reproducing the
102 spatial and temporal variability of VOC emission speciation. Indeed, the emission composition can change depending
103 on the emission source, fuel quality, combustion technologies, and main regional practices (Huang et al., 2017). The
104 use of activity data and emission factors derived from local measurements of regional-specific sources may help to
105 reduce the uncertainties in those emission inventories. In a recent study calculated the emission factors (EFs) of
106 different compounds and activities in southern West Africa (Keita et al., 2018). A comparison of the emissions
107 calculated from the EFs with those observed from the EDGARv4.3.2 (Huang et al., 2017) inventory showed a marked
108 discrepancy (factor of 50 difference) for fifteen VOCs species (3 alkanes, 8 aromatics, isoprene and 3 monoterpenes)
109 in Côte d'Ivoire. That study emphasised the importance of considering African anthropogenic emissions at regional
110 scales. Due to the scarcity of suitable data, the uncertainties in the observations cannot currently be assessed and
111 more detailed studies are required to quantify these uncertainties. Characterization and quantification of the emissions
112 is crucial for improving our understanding of the contributions of anthropogenic and natural sources to the
113 atmospheric composition over southern West Africa, and for assessing their impact on public health and air quality
114 conditions.

115 Several intensive field campaigns in the framework of the Dynamics-Aerosol-Chemistry-Cloud-Interactions in West
116 Africa (DACCIWA) project were conducted in 2015 and 2016 (Knippertz et al., 2015a). Here, we present the results
117 obtained from the VOC field campaigns at different sites, including ambient and near-source measurements, in one
118 of the major southern West Africa cities: Abidjan in Côte d'Ivoire. Abidjan is the economic capital of Côte d'Ivoire
119 with a population of 6.5 million (in 2016), representing more than 20 % of the population of the country (United
120 Nations, 2017). Along with autonomous districts, Abidjan encompasses an area of 2119 km² and is distinguished by
121 remarkable industrialization and urbanization. In summer, West Africa is influenced by monsoon phenomenon which
122 is mainly driven by the surface pressure contrast between the relatively cold waters of the tropical Atlantic Ocean
123 and the Saharan heat low (Knippertz et al., 2017). This seasonal circulation characterized the wet (summer) and dry
124 (winter) periods in the region. During the dry season (November to February), most of the region is dominated by
125 dry northeasterly winds from the Sahara and the precipitation is confined to the coast, where the sea-breeze circulation
126 provides humid air and produces near-surface convergence. Then, the monsoon starts its development and
127 southwesterly moist winds begin to enter deeper into the continent producing more clouds and precipitation between
128 July and August. The strong pressure and temperature gradients between the Atlantic Ocean and the Sahara drive the
129 strong monsoon flow northward along with southwesterlies, reaching higher latitudes up to 20° N (Knippertz et al.,
130 2015b).

131 Speciated VOCs were collected during DACCIWA using sorbent tubes, and then analysed and quantified at the
132 laboratory applying different gas chromatography techniques. These data provide the first constraints for the
133 construction of a regional emission inventory and for understanding the role of anthropogenic VOC emissions in
134 regional atmospheric chemistry.

135 This work aims to establish and analyse the spatial distribution of VOC concentrations and VOC speciated profiles
136 of primary anthropogenic sources in Abidjan by performing sampling under real-conditions. These sources include
137 traditional and regional-specific ones, such as road transportation (gasoline and diesel emissions from different
138 vehicles), charcoal fabrication, and burning emissions from domestic cooking fires, landfill waste, and hardwood
139 fuel. This new dataset provides substantial information enabling the quantification of VOC emissions for several
140 sources in Côte d'Ivoire. These source profiles are analysed and contrasted with those provided by global emission
141 inventories. Finally, the impact on air quality due to the use of regional-specific sources is assessed in terms of
142 reactivity and secondary pollutant formation.

143

144 **2. Materials and Methods**

145 As part of the DACCIWA project, intensive field campaigns were performed in 2015 and 2016, focusing for the first
146 time on the most populated southern coastal region of West Africa. The DACCIWA campaign had an emphasis on
147 atmospheric composition, including air pollution, health impacts and cloud-aerosol interactions (Knippertz et al.,
148 2015a). Here we present new results from intensive ambient measurements in Abidjan and an extended VOC
149 speciation from source emission measurements. These results are part of the activities developed under the
150 workpackage 2 (WP2) - Air Pollution and Health - which aims to link and quantify emission sources, air pollution
151 and related health impacts over different urban sources in West Africa (Knippertz et al., 2015a).

152

153

154 2.1 Sampling

155 The field campaigns were conducted in Abidjan, Côte d'Ivoire during summer and winter according to the strategic
156 directions of the DACCIWA WP2. Two types of cartridges were deployed for VOC measurements: single sorbent
157 cartridge made of Tenax TA 60-80 mesh (250 mg) or multi-sorbent cartridges made of Carbopack B (200mg) and
158 Carbopack C (200 mg (carbotrap 202) purchased from Perkin Elmer). The combination of different sorbent materials
159 allowed the sampling of 10 aromatics (C₆-C₉), 22 n-alkanes (C₅-C₁₆), 10 monoterpenes, 7 aldehydes, isoprene, and
160 other oxygenated compounds. All compounds are reported in Table S1. Before the sampling, cartridges were
161 conditioned by flowing purified nitrogen, at a rate of 100 mL min⁻¹ for 5 hours at 320°C.

162 Firstly, ambient VOC were collected to analyse their spatial distribution in Abidjan. Ambient measurements were
163 performed at nine sites, which are shown in Figure 1. The distribution of the sampling locations was selected
164 according to the primary source locations. They include urban background sites and areas impacted by residential,
165 road transport, domestic fires, waste burning and industrial activities. The characteristics and geographical location
166 of each site are reported in Table 2. The ambient campaigns were conducted during the dry season (February 2016).
167 Samples were collected every 2 days at different times of the day (from 6 a.m. to 8 p.m.) by using a manual pump
168 (Accuro 2000, Dräger) at 100 sccm (standard cubic centimetres per minute) flow rate. One single sorbent tube was
169 exposed six times at each sampling location. In total, 3.6 L of air were collected at each site for a single 600 mL
170 volume each time. Details on the sampling strategy are reported in Table S3.

171 Secondly, direct source emission measurements were performed to obtain VOC emission profiles from the main
172 anthropogenic sources in Abidjan. The sources include traditional ones like road transportation, and southern West
173 Africa specific ones such as domestic waste burning, charcoal fabrication, charcoal burning as well as wood fuel
174 burning (Table 1). Despite that part of these measurements for a limited number of VOC (fifteen species including 3
175 alkanes, 8 aromatics, 3 terpenes and isoprene) and particles were discussed somewhere (Keita et al., 2018), we
176 improve the VOC database extended to 56 VOC species measured in the follow source emissions:

- 177 - For road transportation, analysis of different vehicle exhaust measurements was carried out. Samples
178 integrate five road transportation sub-categories: heavy-duty diesel vehicles (HDDV, trucks, and buses – 3
179 samples on Tenax and 3 samples on Carbopack tubes), light-duty diesel vehicles (LDDV, diesel cars, 2
180 samples on Tenax tubes), light-duty gasoline vehicles (LDGV, gasoline cars, 2 samples on Tenax tubes),
181 two-wheel two-stroke (TW2T, 3 samples on Tenax and 3 samples on Carbopack tubes) and two-wheel four-
182 stroke (TW4T, 3 samples on Tenax and 3 samples on Carbopack tubes) vehicles. Differences in fuel type
183 (gasoline and diesel) and the fleet age have been considered. In African countries, two-wheel vehicles (two-
184 stroke or four-stroke engines) frequently use a mixture of oil and gasoline derived from smuggling, which is
185 characterized by high pollutant emissions (Assamoi and Liousse, 2010).
- 186 - Regarding domestic waste burning (WB), samples were obtained (5 samples on Tenax tubes) at the official
187 domestic landfill site located to the east of Abidjan (AD, Figure 1 and Table 2). The sampling was performed
188 inside the waste burning plume to integrate the different combustion processes involved.
- 189 - Charcoal burning (CH) and wood fuel burning (FW) are common cooking and heating practices in African
190 urban areas. Wood fuel burning emissions were obtained by measuring the fire plume of tropical African
191 hardwood, specifically *Hevea* (*Hevea brasiliensis*). Wood and charcoal were burned in two types of stoves
192 traditionally used in the southern West Africa region for cooking, which are made of metal and baked earth.

193 The measurements included all the combustion phases (Keita et al., 2018) (4 samples on Tenax and 3 samples
194 on Carbopack tubes).

195 – The charcoal making (CHM) profile was obtained by measuring emissions from traditional kilns, that use
196 different types of dense wood. The kiln was covered with a layer of leaves and another one of soil of about
197 10 cm thickness. The smoke was sampled through holes made in the CHM kiln, which are located in the
198 horizontal plane, and provide the air circulation for the pyrolysis propagation (Keita et al., 2018) (2 samples
199 one on Tenax and one on Carbopack tubes).

200 All samples were obtained in the emission plume at around 1–1.5m from the source, except for vehicles where
201 samples were taken at the tailpipe outlet while the vehicle's engine was idling. Carbon monoxide (CO) and carbon
202 dioxide (CO₂) measurements were also performed on the emission sources together with the VOC measurements.
203 For this, the QTRAK-7575 sensor (TSI, Keita et al., 2018) was used to measure real-time CO₂ and CO gas
204 concentrations. CO is measured by using an electrochemical sensor with a sensitivity of 0 to 500 ppm with ±3%
205 accuracy. CO₂ concentrations are obtained by using a non-dispersive infrared detector with a sensitivity of 0 to 5000
206 ppm with an accuracy of ±3 %. The instrument was calibrated in the laboratory prior to each emission measurement
207 These concentrations were used for the estimation of EF values from different samples, which were later averaged
208 for every source category. Details on the sampling strategy at emission are reported in Table S4.

209

210 2.2 Analytical instrumentation

211 Duplicate measurements were performed and analysed in two different laboratories to investigate the reproducibility
212 of analytical techniques and to acquire a wider range of VOC species. The analysis of the Tenax TA tubes was
213 performed at the *Laboratoire de Météorologie Physique* (LaMP, Clermont-Ferrand, France) using a gas
214 chromatograph mass spectrometer system (GC/MS, Turbomass Clarus 600, Perkin Elmer®) coupled to automatic
215 thermal desorption (Turbomatrix ATD). Each tube was desorbed at 270°C for 15 min at a flow rate of 40 mL min⁻¹
216 and pre-concentrated on a second trap, at -30°C containing Tenax TA. After the cryofocusing, the trap was rapidly
217 heated to 300°C (40° s⁻¹) and the target compounds were flushed into the GC. Due to the high loads in some samples,
218 an inlet and outlet split of 5 mL min⁻¹ and 2 mL min⁻¹ were set up, respectively. The analytical column was a PE-
219 5MS (5% phenyl – 95% PDMS, 60m×0.25mm×0.25µm) capillary column (Perkin Elmer) and a temperature ramp
220 was applied to guarantee the VOCs separation (35°C for 5 minutes, heating at 8°C min⁻¹ to 250°C, hold for 2
221 minutes). The mass spectrometer was operated in a Total Ion Current (TIC) from 35 to 350 m/z amu. Chromatography
222 parameters were optimized to enable good separation of fifteen identified compounds by a complete run of 34
223 minutes on each cartridge. Calibration was performed by analysing conditioned cartridges doped with known masses
224 of each compound, present in certified standard low-ppb gaseous standard, purchased from the National Physical
225 Laboratory (NPL, UK; 4 ppb ±0.8 ppb). That method provided the separation and identification of 16 compounds,
226 from C₅ to C₁₀ VOCs, including 8 aromatics, 3 monoterpenes, 4 alkanes and isoprene. The limit of detection lies
227 between 1.10 ppt (1,2,3-trimethylbenzene) and 22.6 ppt (2-methylpentane). The global uncertainty is estimated
228 between 5% and 38%.

229 Carbopack tubes analysis was carried out by applying a gas chromatography-flame ionization detector (ATD-GC-
230 FID, Perkin Elmer) system at the *SAGE Department (IMT Lille Douai)*. The cartridges were previously thermo-
231 desorbed at 350°C for 15 minutes with a helium flow of 20 mL min⁻¹. This method allowed the separation and

232 identification of up to 56 compounds, from C₅–C₁₆ VOCs, including 7 aldehydes, 4 ketones, 10 monoterpenes and 6
233 long-chain alkanes from C₁₂ to C₁₆. More details on the analytical technique can be found elsewhere (Ait-Helal et
234 al., 2014; Detournay et al., 2011). VOCs can be classified according to their saturation concentration, C*, which
235 indicates their volatility (Ait-Helal et al., 2014; Epstein et al., 2010; Robinson et al., 2007). Here, C₁₂–C₁₆ alkanes
236 are classified as VOC of intermediate volatility, since given their C* values are between 10³ μg m⁻³ <C* < 10⁶ μg m⁻³
237 (Ait-Helal et al., 2014). The detection limits lie between 1 ppt to 13 ppt (hexadecanal) and the global uncertainty
238 varies between 3.7% and 32.6% as detailed elsewhere (Detournay et al., 2011; Keita et al., 2018).

239 The application of both methods allowed the comparison of common compounds that were measured at ambient sites
240 and sources (benzene, toluene, ethylbenzene, m+p-xylene, o-xylene, trimethylbenzenes, n-heptane, iso-octane, n-
241 octane, α-pinene, β-pinene, limonene, isoprene) and the performance analysis of the analytical techniques.
242 Furthermore, the combination of different sorbent tubes and analytical strategies allowed the quantification of a
243 higher number of VOC species, and therefore, a more extensive analysis of source contributions.

244

245 2.3 Metrics and calculations

246 Different calculations were implemented to assess the VOC emissions and their impacts in Abidjan. Here we provide
247 the mathematical basis for each investigated parameter. Firstly, the emission factors (EF) were computed for the
248 whole extended VOC database (56 compounds) following the methodology described in Keita et al. (2018). EFs
249 combined with regional statistics were later used for the estimation of VOC emissions in Côte d'Ivoire for each
250 source category. Secondly, the emission ratios (ER) of each VOC species related to CO for all the emission sources
251 were established. Finally, the reported ERs were used to evaluate the impacts on atmospheric reactivity by applying
252 commonly used metrics.

253

254 2.3.1 Emission factors and quantification of VOC emissions

255 VOC emission factors were estimated from the concentrations measured for all the emission sources, as follows

$$256 \quad EF(VOC) = \frac{\frac{\Delta VOC}{\Delta CO + \Delta CO_2} \times MW_{VOC}}{12} \times fc \times 10^3 \quad (1)$$

257 where EF (VOC) is the emission factor of the specific VOC in gram per kilogram of burned fuel (g kg⁻¹); ΔVOC =
258 [VOC]_{emission} – [VOC]_{background} is the VOC mixing ratio in the emission and background air respectively, in parts per
259 billion by volume (ppbv), MW_{VOC} is the molar weight of the specific VOC (in g mol⁻¹), 12 is the molar weight of
260 carbon (g mol⁻¹) and *fc* is the mass fraction of carbon in the fuel analysed. The *fc* values used were obtained from the
261 literature and applied to each source. The EF for selected fifteen VOCs were already published and more details
262 about the method can be found elsewhere (Keita et al., 2018). Here we applied the same method for the whole VOC
263 database, including 56 compounds directly measured from the emission sources. For this, VOC emissions were
264 estimated using the emission factors obtained from near-source measurements along with the statistical International
265 Energy Agency (IEA) activity data, available for the different sources). Equation 1 was used to compute the emission
266 factors, considering all the VOC species measured and including the mass fraction of each fuel (*fc*) obtained from
267 the literature. Additionally, the differences in fuel type and the fleet age have been considered, as well as the fleet
268 distribution by calculating the equivalent vehicular fleet. For the road transport sector, the equivalent fleet means
269 were calculated considering the fleet characteristics in Côte d'Ivoire, as detailed in Keita et al. (2018). These

270 calculations were based on the information given by the Direction Generale des Transports Terrestres in Côte
271 d'Ivoire, which considered that 60% of vehicles are old models and 77% of the total fleet is composed by light-duty
272 vehicles. Regarding two-wheel vehicles, 60% of them are two-stroke engines and only 40% of the total are considered
273 as recent vehicles (SIE CI, 2010). In the residential profile, we integrated the emissions measured from charcoal
274 making, charcoal burning and wood fuel burning sources, commonly observed at residential sites in Abidjan.
275 Afterwards, the mean road transportation and residential profiles for Côte d'Ivoire were computed and compared
276 with two referenced global inventories, EDGAR v4.3.2 and MACCity (Granier et al., 2011; Huang et al., 2017).

277

278 2.3.2 Molar mass emission ratios

279 Emission ratios (ER) were obtained by dividing each VOC mixing ratio by carbon monoxide (CO) mixing ratios as
280 follows:

$$281 \quad ER = \frac{[\Delta VOC] \text{ ppbv}}{[\Delta CO] \text{ ppmv}} \quad (2)$$

282 We selected CO as a combustion tracer because most VOCs and CO are co-emitted by the target sources.
283 Furthermore, ratios to CO are regularly reported in the literature for biomass burning and urban emissions (Baker et
284 al., 2008; Borbon et al., 2013; Brito et al., 2015; Gilman et al., 2015; de Gouw et al., 2017; Koss et al., 2018; Wang
285 et al., 2014) which are useful constraints for further comparisons. Emission ratios were calculated in ppbv of VOC
286 per parts per million by volume (ppmv) of CO, which is similar to a molar ratio (mmol VOC per mol CO). Molar
287 mass (MM) emission ratios were also computed following Gilman et al. (2015). MM is the VOC mass emitted (μg
288 m^{-3}) per ppmv CO, obtained from equation 2 and converted by using the VOC molecular weight (MW) (g mol^{-1})
289 and the molar volume (24.86 L at 1 atm and 30°C). Table S1 includes the emission ratios obtained for each VOC and
290 MW values used.

291

292 2.3.3 VOC-OH reactivity

293 The OH reactivity was estimated to evaluate the potential contribution of each measured VOC to the photochemical
294 processing. VOC-OH reactivity represents the sink reaction of each VOC with the hydroxyl radical (OH) and is equal
295 to

296

$$297 \quad VOC_{OH \text{ reactivity}} = ER \times k_{OH} \times CF, \quad (3)$$

298 where ER is the emission ratio for each VOC related to CO (ppbv per ppmv), k_{OH} is the second-order reaction rate
299 coefficient of VOC with the hydroxyl radical ($\times 10^{-12} \text{ cm}^3 \text{ molecule}^{-1} \text{ s}^{-1}$) and CF is the conversion factor of molar
300 concentration ($2.46 \times 10^{10} \text{ molecule cm}^{-3} \text{ ppbv}^{-1}$ at 1 atm and 25°C) (Gilman et al., 2015). k_{OH} values for all VOC
301 species were obtained from Atkinson and Arey (2003) and the NIST Chemical Kinetics Database (Manion et al.,
302 2015).

303

304 2.3.4 Ozone Formation Potential

305 The oxidation of VOCs is often initiated by the reaction with the hydroxyl radical ($\cdot\text{OH}$), which in the presence of
306 NO_x ($\text{NO} + \text{NO}_2$) leads to the photochemical formation of O_3 . The ozone formation potential represents the ability of
307 each VOC to produce tropospheric ozone and it was calculated as follows:

308

309
$$VOC_ozone\ formation\ potential = ER \times POCP, \quad (4)$$

310 where the ER is the emission ratio of each VOC related to CO (ppbv of VOC per ppmv of CO) and POCP is the
311 photochemical ozone creation potentials developed in previous studies (Derwent et al., 2007; Jenkin et al., 2017).
312 POCP values were obtained by simulating a realistic urban mass trajectory with the Master Chemical Mechanism
313 (MCM). This model estimates the change in ozone production by incrementing the mass emission of each VOC
314 (Derwent et al., 1998). POCPs for an individual VOC are estimated by quantifying the effect of a small increase in
315 its emission on the concentration of the formed modelled ozone, respective to that resulting from the same increase
316 in the ethene emission (POCP value for ethene is, therefore, 100). In this study, POCP values were analysed on VOC
317 family basis obtained from a recent study (Huang et al., 2017), or adapted from individual POCP values.

318

319 2.3.5 Secondary organic aerosol (SOA) formation potential

320 The SOA formation potential represents the propensity of each VOC to form secondary organic aerosols and is equal
321 to

322
$$SOA_VOC\ formation\ potential = ER \times SOAP, \quad (5)$$

323 where ER is the emission ratio for each measured VOC related to CO (ppbv of VOC per ppmv of CO) and SOAP is
324 a non-dimensional model-derived SOA formation potential (Derwent et al., 2010; Gilman et al., 2015). All SOAP
325 values represent the modelled mass of organic aerosol that were formed per mass of VOC reacted on an equal mass
326 emitted basis relative to toluene. Toluene was selected as the reference compound due to its well-known emissions
327 and it is usually documented as a critical anthropogenic SOA precursor (Derwent et al., 2010).

328

329 ER, k_{OH} and SOAP values for each VOC and each source are detailed in Table S1. In the absence of SOAP values
330 for specific compounds, we estimated the values (indicated in Table S1, referred as ^a) by using those of comparable
331 compounds based on similar chemical properties, as suggested in the study of Gilman et al. (2015).

332

333 2.4 Ancillary data

334 Meteorological observations were provided by the NOAA Integrated Surface Database (ISD; <https://www.ncdc.noaa.gov/isd> for more details). Daily rainfall, air temperature, and wind speed and direction measurements
335 were recorded at the Abidjan Felix Houphouet Boigny Airport. Figure 1 gives the geographical location of the
336 meteorological station and ambient sampling locations.

338

339 3. Results and discussion

340 3.1 Local meteorological conditions

341 Meteorological data from Abidjan, Côte d'Ivoire, are reported in Figure 2. Weekly accumulated precipitation and
342 weekly air temperature means were analysed during 2016. Meteorological conditions in Abidjan are also affected by
343 the monsoon phenomenon which establishes two well defined seasons: a wet season between March and August and
344 a dry season from November to February. The weekly mean air temperature observed was between 24.6 and 29.4°C,
345 reaching a maximum during the beginning of the wet season (Figure 2). The precipitation pattern shows an increased
346 rate during the monsoon period; however, negative anomalies were observed this year compared with the previous

347 ones (Knippertz et al., 2017). Observed wind patterns during the field campaign showed a predominant contribution
348 from the southwesterly sector with maximum speed during daytime up to 13 m s^{-1} . The high wind speed records
349 reported in Abidjan are higher than those observed in other polluted urban atmospheres (Dominutti et al., 2016;
350 Salameh et al., 2016a; Zhang et al., 2014).

351

352 3.2 VOCs in Abidjan atmosphere

353 Our analysis relies on the fifteen VOC species already listed in Keita et al. (2018, only for emission sources) and
354 these were measured in both ambient air and at emission sources. The VOCs include 8 aromatic hydrocarbons, 3
355 monoterpenes, 3 alkanes, and isoprene which span a wide range of reactivity and represent the various types of VOC
356 expected to be released by fossil/non-fossil fuel combustion and biogenic emissions.

357

358 3.2.1. Ambient concentrations and spatial distribution

359 The ambient concentration sum of the fifteen quantified VOCs ranged from 6.25 to $72.13 \mu\text{g m}^{-3}$ (see size-coded pie
360 chart, Figure 3). Higher VOC concentrations were reported in KSI, BIN CRE and PL sites (Figure 3). The
361 predominant VOCs are toluene ($4.18 \pm 3.55 \mu\text{g m}^{-3}$), m+p-xylene ($4.05 \pm 3.41 \mu\text{g m}^{-3}$), iso-octane ($2.59 \pm 3.37 \mu\text{g}$
362 m^{-3}), benzene ($1.00 \pm 0.41 \mu\text{g m}^{-3}$), ethylbenzene ($0.93 \pm 0.86 \mu\text{g m}^{-3}$) and limonene ($0.77 \pm 0.76 \mu\text{g m}^{-3}$). Overall,
363 anthropogenic VOCs dominated the ambient composition by a factor of 5 to 20 compared to biogenic ones. BTEX
364 (benzene, toluene, ethylbenzene, and m+p and o-xylenes), a subgroup of aromatic VOCs, usually makes up a
365 significant fraction of the VOC burden in urban atmosphere (Borbon et al., 2018; Boynard et al., 2014; Dominutti et
366 al., 2016). They are emitted by fossil fuel combustion from transport and residential sources as well as evaporation
367 processes such as fuel storage and solvent uses (Borbon et al., 2018). Here their contribution ranged from 35% to
368 76% of the total VOC burden measured at the ambient sites. Therefore, the following discussion will only focus on
369 BTEX as representative of all measured anthropogenic VOC patterns. Figure 3 shows the spatial distribution of the
370 total VOC concentrations at each site and detailed by the BTEX composition. Firstly, a spatial heterogeneity of the
371 total measured VOC concentration (total values on pie chart, Figure 3) is depicted in the Abidjan district. This spatial
372 heterogeneity has been already pointed out by recent studies performed in Abidjan for other atmospheric pollutants
373 (Bahino et al., 2018; Djossou et al., 2018). While a spatial heterogeneity was also observed in aerosol concentrations
374 (Djossou et al., 2018), maximum aerosol concentrations were reported near domestic fires (similar to KSI) and
375 landfill sites (AD), showing a different pattern than the one observed for the VOC concentrations. Besides the dilution
376 processes, the spatial distribution of total VOC concentrations seems to be related to the proximity of emission
377 sources, affecting ambient VOC concentrations in the different sampling locations. For example, higher total VOC
378 concentrations were mainly observed in the central urban area (like KSI, CRE and PL) where the density of emission
379 sources increases.

380 Second, m+p-xylene and toluene dominate the ambient distribution of BTEX, ranging from 9 to 27 % and 8 to 31 %
381 of the total VOC, respectively. BTEX composition is consistent between PL, CRE, BIN and KSI sites with high VOC
382 loads while an enrichment in benzene concentrations is observed at FAC, ABO, ZYOP, AT and AD sites (from 16%
383 to 30% contribution). The BTEX composition can be affected by emissions and chemistry. The toluene-to-benzene
384 ratio is a useful indicator of either traffic and non-traffic source or chemistry effects. On the one hand, the toluene-
385 to-benzene at PL, CRE, BIN and KSI sites is higher than 4 which suggests the influence of sources other than traffic

386 like industrial sources. On the other hand, the toluene-to-benzene lie between 0.8 and 1.9 at lower VOC load sites
387 (FAC, ABO, ZYOP, AT and AD) (Brocco et al., 1997; Heeb et al., 2000; Muezzinoglu et al., 2001). These values
388 are closer to the one usually observed at traffic emissions. There is no visible effect of chemistry here especially on
389 higher aromatics like C8-aromatics with a shorter lifetime whose contribution stays almost constant regardless of the
390 site.

391 The mean ambient concentrations observed in Abidjan for alkanes and aromatics were compared with those observed
392 in other cities worldwide (Figure 4). On one hand, mean concentrations in Abidjan depicted lower values when
393 compared with those measured in other cities (Figure 4). Keita and co-workers (2018) pointed out the high emissions
394 observed in Abidjan sources. In their study, road transport and wood burning VOC emission factors spanned 2 to 100
395 orders of magnitude, respectively, when compared with those from the literature. Our ambient observations suggest
396 that wind speed have an important role in the mixing and dilution of the anthropogenic emissions leading to low
397 VOC concentrations in the Abidjan atmosphere. As it was pointed out in the meteorological description, the proximity
398 of Abidjan to the ocean and the intrusion of the sea-breeze circulation can facilitate the dispersion processes and,
399 consequently, the urban emissions dilution. Indeed, Deroubaix et al. (2019) analysed the regional dispersion of urban
400 plumes from southern West Africa coastal cities, i.e. Abidjan, where the inland northward transport of anthropogenic
401 coastal pollutants along with biomass burning emissions were observed.

402 On the other hand, a reasonably good agreement in the relative composition of alkanes and aromatics is observed,
403 showing the same distribution in most cities, except for Karachi where higher contributions of heptane and benzene
404 were measured (Barletta et al., 2002). Observed concentrations of hydrocarbons result from primary emissions,
405 chemical processing and dilution in the atmosphere. Dilution affects equally all the compounds by decreasing
406 absolute levels without altering their composition. Chemistry can be neglected because the transport time between
407 major urban sources and receptor sites is usually less than the compound lifetimes (here the shortest lifetime for
408 trimethylbenzene is 4.3h). Finally, only emissions are expected to significantly alter the hydrocarbon composition.
409 However, the composition is the same regardless of the location. Such commonality suggests that the urban
410 hydrocarbon composition worldwide is controlled by emissions from fossil fuel combustion and, gasoline powered
411 vehicle in particular (see also next section). Finally, the ambient hydrocarbon distributions in Abidjan are noticeably
412 similar to other northern mid-latitude megacities, suggesting that emissions from fossil fuel combustion for alkanes
413 and aromatics dominate over other regional-specific sources. These results are also consistent with previous studies
414 comparing different database worldwide without including an African city like Abidjan (Borbon et al., 2002;
415 Dominutti et al., 2016; von Schneidemesser et al., 2010). Even if emissions can be different in intensity (number of
416 vehicles for instance), the hydrocarbon composition seems to be similar in the different urban atmospheres.

417

418 3.2.2. Ambient composition vs. emission source profiles

419 A comparative approach was carried out between ambient and source measurement compositions with the purpose
420 of detecting emission source fingerprints in ambient VOC profiles. Figure 5 shows the relative mass contribution of
421 VOC profiles observed at the nine urban sites together with those obtained from the emission sources. While a
422 noticeable variability in the contribution of emission sources is observed, smoother differences are depicted between
423 the ambient sites. This result reinforces the similar BTEX profiles discussed in the section 3.2.1, where the mixing
424 and dilution process were suggested as the main drivers in the control of ambient emissions. Trimethylbenzenes (124-

425 TMB, 135-TMB, and 123-TMB), mainly observed in road transport emissions, display a dissimilar profile showing
426 higher fractions from sources than ambient sites (Figure 5). These differences might be related to the short lifetime
427 of these compounds (around 4 hours), with a reaction rate ranging from 1.8 to $8.8 \times 10^{-15} \text{ cm}^3 \text{ molecule}^{-1} \text{ s}^{-1}$ (Atkinson
428 and Arey, 2003). Their reactivity implies a faster reaction in the atmosphere and losses of these species from the
429 emission to the receptor.

430 On the other hand, in most of the cases, ambient profiles showed higher contributions of alkanes, monoterpenes and
431 isoprene, likely associated with the contribution from different anthropogenic and biogenic sources. The presence of
432 terpenes and isoprene in the profile of all emission sources is notable, mainly in those associated with domestic
433 burning processes, such as charcoal, waste and wood fuel burnings (Figure 5). The terpene emissions from biomass
434 burning were already identified in several studies as they are common species emitted by combustion processes
435 (Gilman et al., 2015; Simpson et al., 2011). Additional studies based on African biomass emissions also reported
436 concentrations of limonene and α -pinene higher than isoprene (Jaars et al., 2016; Saxton et al., 2007).

437 For the selected VOC species, aromatic compounds represent the higher fraction from ambient and source profiles,
438 contributing from 31 to 75% (Figure 5). Comparing the same VOC species in emission sources versus ambient
439 profiles, we found a similarity with the two-wheel vehicle and domestic fire profiles like wood fuel burning and
440 charcoal burning sources. Nevertheless, the VOC ambient profiles obtained from the sites did not show a contrasted
441 difference despite the differences in the activities conducted nearby.

442

443 3.3. Molar mass of measured VOC emissions in Abidjan.

444 Here we compare the composition and magnitude of anthropogenic emissions as a function of molar mass emission
445 ratios as described in section 2.3.2, which is a readily calculated property used to quantify anthropogenic emissions
446 (Gilman et al., 2015). For this analysis, our expanded VOC database of 56 species was considered, including 12
447 terpenes, VOCs of intermediate volatility (IVOCs from C_{12} – C_{16} n-alkanes), ketones and aldehydes ($>C_6$) compounds
448 for all sources (Table 1 and Table S1). Species groups were classified according to GEIA groups (Huang et al., 2017)
449 according to the chemical function of each VOC family (Table S2). In this way, molar masses were also grouped by
450 VOC family from individual values (Table S1). Since the VOCs of intermediate volatility (IVOCs) do not have a
451 specific classification, they were integrated in the group of heavy alkanes (VOC6). Note also that the most volatile
452 fraction of OVOC which usually represents the major fraction, is not represented here in the VOC22 and VOC23
453 categories. The associated contribution should be analysed as the lower expected limit. Figure 6 shows the
454 contribution of VOC groups to the measured molar mass and the total molar mass of each source, while Figure 7a-d
455 (upper panel) compared the magnitude of measured molar masses for the four leading sectors. As already described
456 in the previous section, the distribution reported in Figure 6 reveals the predominance of aromatic molar masses
457 (VOC13-VOC17), ranging from 26 % to 98 %. The prevalence of these compounds is predominantly observed in
458 gasoline-fuelled vehicles, like gasoline light-duty (LDGV) and two-wheel (TW) vehicles and diesel light-duty
459 vehicles (LDDV). Alkanes (VOC5+VOC6) also comprise a noticeable molar mass fraction, dominating in two-wheel
460 two-stroke vehicle, heavy-duty vehicle and charcoal related sources (by 40, 47 and 53%, respectively).

461 A considerable IVOCs contribution from the emission of heavy-duty vehicles was observed, with IVOCs dominating
462 the VOC6 fraction by 30% (considering that VOC6 represents 47% of the total emissions from this source).

463 Interestingly, and as already discussed in Section 3.2.2, monoterpenes (VOC11) comprised 11%, 13% and 22%
464 contribution in wood fuel burning, heavy-duty vehicle and waste burning sources, respectively (FW, HDDV and WB,
465 Figure 6 and Figure 7b-c). Terpenes in biomass burning sources were already pointed out as the most significant
466 emitted compounds together with furans and aromatics in chamber experiments (Koss et al., 2018). Nevertheless, to
467 the extent of our knowledge, their presence in road transport or open waste burning emissions remains unexplored.
468 Regarding OVOCs (VOC22), they were observed in a smaller fraction (less than 7%) apart from heavy-duty vehicles,
469 which contributes to 11% of the total measured molar mass. Previous studies have reported OVOCs as the main
470 fraction in biomass burning emissions (Akagi et al., 2011; Gilman et al., 2015; Yokelson et al., 2013). Moreover,
471 Sekimoto and co-workers also analysed the VOC emission profiles depending on the pyrolysis temperature, showing
472 enrichment of terpenes and non-aromatic oxygenates under high-temperature conditions and an increase in
473 oxygenated aromatics under low-temperature fires (Sekimoto et al., 2018). Comparing the burning-related sources
474 such as wood fuel burning with previous studies, a lower total measured molar mass was observed in our study than
475 those obtained in the US fuels, by a factor of 33 to 117 (Gilman et al., 2015). In that work, Gilman and co-workers
476 have shown that OVOCs represent 57 to 68% of the total measured molar mass. A different pattern is observed in
477 this study, likely related to the limitation of VOC species measurements by the sampling method deployed, which
478 allows the collection of a limited number of aldehydes ($>C_6$) and other oxygenated compounds as well. Thus, our
479 total molar mass estimation for the sources in Abidjan should be considered as lower limit since additional
480 contributions could be expected from other unknown emitted VOCs, such as OVOCs, alkenes and nitrogenated
481 VOCs.

482 Four sources (TW2T, HDDV, WB, and CH) that represent the leading sectors in the region (road transportation,
483 waste burning, and charcoal burning emissions) were selected, in order to analyse the magnitude of emissions as a
484 function of molar mass and their potential impacts related to African emissions (next section). Figure 7 (a-d) shows
485 the relative composition and the total molar mass of the measured VOC ($\mu\text{g m}^{-3}$) emitted per ppmv of CO. Two-
486 wheel two-stroke vehicles (TW2T) disclosed the highest molar mass emissions ($4680 \pm 512 \mu\text{g m}^{-3} \text{ ppmv CO}^{-1}$,
487 Figure 7a-d). TW2T emissions were 10 to 200 times higher than any other source here analysed, such as heavy-duty
488 vehicle ($458 \pm 60 \mu\text{g m}^{-3} \text{ ppmv CO}^{-1}$), wood fuel burning ($31.5 \pm 2.50 \mu\text{g m}^{-3} \text{ ppmv CO}^{-1}$), charcoal burning (43.8 ± 6.37
489 $\mu\text{g m}^{-3} \text{ ppmv CO}^{-1}$) and light-duty vehicle ($137.5 \pm 20 \mu\text{g m}^{-3} \text{ ppmv CO}^{-1}$) emissions (Figure 6). While aromatics
490 (VOC13-VOC17) seem to dominate the molar mass fraction for most sources, their contributions are dissimilar,
491 dominated by benzene (VOC13) and toluene (VOC14) in burning-related sources, and by xylenes (VOC15) and
492 trimethylbenzenes (VOC16) in traffic-related ones.

493

494 3.4 Implications on atmospheric reactivity

495 The estimation of the impact on atmospheric chemistry of measured VOC emissions is based in the three metrics
496 described in the Section 2.3.

497

498 3.4.1 OH reactivity of measured VOC emissions

499 Figure 7(e-h) shows the fractional contributions and total VOC-OH reactivity per ppmv of CO for the selected
500 sources. The highest total reactivity is observed from the emissions of two-wheel two-stroke vehicles (TW2T, $488 \pm$
501 $43 \text{ s}^{-1} \text{ ppmv CO}^{-1}$), outpacing other sources by a factor of 7 to 170. This disclosed difference is related to the high

502 ERs observed for the more reactive species, like terpenes (VOC11) and C₈- and C₉-aromatics (VOC15 and VOC16,
503 respectively). Terpenes (VOC11) and aromatics (VOC13-VOC17) altogether are the dominant sink of OH,
504 contributing to 47 to 87% of the total calculated OH reactivity. Individually, terpenes governed the OH reactivity in
505 open waste burning emissions (76%) and heavy-duty diesel vehicles (60%) (Figure 7f-g). When compared with other
506 sources, a singular profile is observed for charcoal burning emissions where aldehydes (VOC22, 13%) and heavier
507 alkanes (VOC6, 28%) have higher contribution than in other emission sources. The modest presence of alkenes in
508 the VOC-OH fractional analysis, well-known for their high reactivity effects, is related to the limitation of the
509 sampling method which does not allow the collection of light alkene species. We might expect a high contribution
510 of alkenes adding to the terpene burden.

511

512 3.4.2 Ozone formation potential of measured VOC emissions

513 Overall, the fractional ozone formation distribution is dominated by aromatics (VOC13 to VOC17) in all sources, by
514 38 to 63%. Alkanes (VOC6) represent a significant contribution in charcoal burning, heavy-duty diesel vehicles, and
515 two-wheel two-stroke vehicles, accounting for 45, 28 and 26%, respectively. It is important to note the terpenes
516 (VOC11) contribution, coming not only from burning sources but also from the road transportation sector (Figure 7i-
517 l). Aldehydes (VOC22) are well-known due to their high reactivity in the atmosphere (Atkinson and Arey, 2003;
518 Sommariva et al., 2011), and some of these species have shown a large impact on ozone formation and chemistry. In
519 our estimation, we can observe the contribution of these compounds mainly from diesel (HDDV) and charcoal
520 burning sources (CH). The total potential ozone was calculated for each source, showing most of the time a dominant
521 contribution from two-wheel two-stroke vehicles (80 343 POCP ppmv CO⁻¹), which is 13, 24 and 150 times higher
522 than the potential impact in ozone formation derived from heavy-duty vehicles, waste burning and charcoal burning
523 emissions, respectively.

524

525 3.4.3 SOA formation potential of measured VOC emissions

526 Figure 7 (m-p) shows the composition and mean SOA formation potentials of VOC families emitted by each selected
527 source. As can be expected, charcoal burning has the lowest SOAP values (335 SOAP per ppmv CO⁻¹), compared
528 with two-wheel two-stroke vehicle, heavy-duty vehicle and waste burning sources, whose SOAPs values are 147, 10
529 and 9 times greater, respectively. Globally, aromatics (VOC13-VOC17) governed the SOA formation in our
530 estimations, by 72 to 98%. Interestingly, terpenes (VOC11) represented a minor contribution in the SOA formation,
531 presenting a SOAP index lower than for aromatic species. It represents approximately 20% of the SOAP for toluene
532 (VOC14). Despite the well-known role of terpenes as SOA precursors (Ait-Helal et al., 2014), the method used here
533 is not able to correctly quantify their contributions to SOA formation. The differences between SOAP values and
534 measured aerosols yield were already pointed out by Gilman and co-authors (Gilman et al., 2015), who performed
535 some sensitivity tests in order to harmonize SOAP and aerosols yields. We performed the same analysis here,
536 adjusting the SOAP terpene values to be 10% higher. The results in total SOAP per ppmv of CO did not show
537 considerable increases in any of the sources, expanding the total SOAP up to 1%. Similar results were observed for
538 fractional distribution, so that the changes in terpenes SOAPs (VOC11) did not show any substantial change in the
539 VOC contribution for SOA formation. These findings are in agreement with those identified in the study of Gilman

540 et al. (2015), suggesting an underestimation in the fractional contribution of terpenes to the potential formation of
541 organic aerosols over southern West Africa region.

542

543 3.5 Quantification of VOC emissions

544 Anthropogenic VOC emissions were quantified by considering the complete VOC dataset, which includes the 56
545 compounds analysed, aldehydes, IVOCs and terpenes species. Mean residential emissions are also integrated and
546 compared with those from the EDGAR v4.3.2 inventory. Additionally, we incorporate the residential and road
547 transport profiles provided by the MACCity inventory (Granier et al., 2011), available in the ECCAD-GEIA database
548 (<http://eccad.aeris-data.fr>). The main differences between both global inventories are related to the speciation level
549 of VOCs families. MACCity considers all the aromatics in the same VOC group; thus, we provide here the sum of
550 VOC13 to VOC17 families (Table S2) to compare it with the aromatics group from our quantification.

551 Figure 8 exhibits the speciated emissions calculated for Côte d'Ivoire along with those provided by the two emission
552 inventories. Globally, the discrepancies already highlighted in the previous analysis are exacerbated by introducing
553 the complete VOC database. Calculated residential emissions are greater by a factor of 14 and 43 when compared
554 with EDGAR v4.3.2 and MACCity, respectively (Figure 8a). In terms of composition, the main differences observed
555 are related to the VOC22 group (aldehydes). This group discloses a higher contribution by a factor of 5 in the EDGAR
556 inventory, accounting for 64% of the total emission. There is also a disparity in the contribution from aromatics (sum
557 of VOC13 to VOC17) and alkenes (VOC12), which reveals a more substantial influence in the MACCity profile
558 (58% and 22%, respectively) (Figure 8a). This disparity could be related to the few VOC species that were analysed
559 for the VOC12 group in our study. Nevertheless, aromatics dominate the fractional contribution in our calculated
560 emissions (39%), especially toluene (VOC14) and C₈-aromatics (VOC15) (11% and 10%, respectively). Alkanes
561 (>VOC6 alkanes) show a more significant contribution in the residential profile, in which IVOCs contribute 20% of
562 the total calculated alkanes obtained by our estimations.

563 Regarding the road transportation sector, total calculated emissions are higher than the global inventories by a factor
564 of 100 and 160 for EDGAR and MACCity, respectively (Figure 8a). A moderate agreement is observed with
565 speciation (Figure 8b). Aromatics and alkanes are the main contributions for all profiles in different proportions. Our
566 estimates report the most significant contributions in C₈-aromatics (VOC15), C₉-aromatics (VOC16) and toluene
567 (VOC14), with a 25, 14 and 10% contribution, respectively (Figure 8c and Figure 9). In comparison, EDGAR v4.3.2
568 shows a contribution of 9% for VOC15, 3.5% for VOC16 and 13% for VOC14 (Figure 9). Road transport profiles
569 also reproduce the anomalies in the VOC12 (alkenes) contribution observed in the residential sector, presenting
570 greater emissions in the global inventories. The comparison between both inventories also depicted considerable
571 discrepancies, of a factor of 3.

572 A similar profile is observed for heavier alkanes (VOC6) which present an analogous contribution between our
573 estimation and EDGAR emissions (34 and 37%, respectively; Figure 8b). Nevertheless, the alkanes (VOC5+VOC6)
574 contribution in the MACCity profiles prevails over road transport emissions accounting for 62% of the total
575 emissions.

576 Interestingly, terpenes and isoprene emissions can be denoted in both sectors in the Côte d'Ivoire calculated emissions
577 (VOC11 and VOC10). Despite the reduced contribution of these species (9% in residential and 4% in road transport),
578 the underestimation of them in the emissions from anthropogenic sources could have consequences for atmospheric

579 chemistry. Since the reactivity is specific for each VOC, the inaccuracies in the speciation could also have
580 implications on the estimation of their impacts. Specifically for terpenes (VOC11), it can be noted their high
581 contribution in the k_{OH} reactivity, accounting for 42% in the residential sector and 28% in road transport sector
582 reactivities (Figure 8c). Even though the total OH reactivity in all profiles is rather similar, the alkenes fraction in
583 this study is not well-represented which could increase the contribution in terms of reactivity.

584 Figure 9 also displays the residential and road transportation profiles obtained from Côte d'Ivoire, compared with
585 EDGAR v4.3.2 profiles for Europe. Noticeably in our estimations, road transport and residential sectors presented
586 comparable total emissions, whereas those from the EDGAR inventory were different by a factor of 8 (86.1 vs 12.1
587 Gg year⁻¹, respectively). Similar disagreements are also observed when comparing EDGAR total emissions for
588 Europe with Côte d'Ivoire, where the former presents larger emissions (198 vs 86 and 433 vs 12 Gg year⁻¹,
589 respectively). We highlight here the substantial differences in total emissions, outpacing those estimated for Europe
590 by a factor of 3 for road transport and by a factor of 6 for residential sector (433 and 198 Gg year⁻¹, respectively).

591 The lack of measurements and source profile data in Africa was previously pointed out in the development of EDGAR
592 inventory, which led to considering the priority of this region for future inventory improvements (Huang et al., 2017).
593 Even though our VOC database is not extensive for all the species emitted by the sources analysed, the incorporation
594 of new VOC species reinforces the usefulness of *in situ* measurements under real conditions to derive realistic
595 emission factors and subsequent estimates of representative emission profiles.

596

597 3.6 Anthropogenic emissions of terpenes, IVOCs and aldehydes in southern West Africa

598 As previously highlighted, terpenes commonly emitted by biogenic sources were observed in the emissions from
599 anthropogenic sources. Global emission inventories wholly neglect these emissions; however, they could have
600 considerable effects in the atmospheric chemical processing, by producing secondary pollutants in the atmosphere.
601 Figure 10a shows the fractional distribution of terpenes in several analysed emission sources. The main contributions
602 are associated with the emissions from waste burning (47%), two-wheel vehicle (20%), wood fuel burning (17%)
603 and charcoal making (14%) sources. The total annual emissions estimated for these compounds, which represents
604 334 Gg year⁻¹ and 11% of the total emissions, cannot be neglected when compared with the emission of other well-
605 known anthropogenic VOC, i.e. C₉-aromatics. Evaluating the distribution of terpene species among the emission
606 sources permits a different pattern to be noted (Figure 11). While terpene emissions from road transport are mainly
607 dominated by α -ocimene and α -terpinolene, limonene and isoprene are mainly emitted by wood-burning sources. The
608 main wood types burnt in Côte d'Ivoire are Hevea (*Hevea brasiliensis*) and Iroko (*Milicia excelsa*), which are widely
609 used in urban domestic fires for cooking, heating and other services (Keita et al., 2018). In our study, we only present
610 the results obtained from Hevea, a tropical African hardwood, characterised as a species that emits monoterpenes
611 (Bracho-Nunez et al., 2013; Wang et al., 2007). The principal monoterpene compounds naturally emitted by Hevea
612 species are sabinene, limonene, and α -pinene (Bracho-Nunez et al., 2013). The isoprene emissions from non-isoprene
613 emitting species were already observed in biomass burning studies, which indicates that isoprene is formed during
614 the combustion process (Hatch et al., 2015).

615 As it can be noted in Figure 11, isoprene emissions are also impacted by vehicles, mainly two-wheel sources, and
616 camphene and β -pinene emissions by heavy-duty vehicle sources. The anthropogenic sources of isoprene have been
617 documented in urban areas, mainly associated with traffic emissions (Borbon et al., 2001; von Schneidmesser et al.,

618 2011). However, to the best of our knowledge, no previous studies have ever analysed the presence of monoterpenes
619 from road transportation sources. α -pinene and β -pinene emissions are dominated by charcoal burning fires, which
620 also contribute in some fraction to the emissions of isoprene and limonene. In contrast, charcoal making emissions
621 are dominated by γ -terpinene and isoprene. The results from biomass burning sources provided here were obtained
622 from non-controlled experiments, which did not allow the evaluation of differences between the emissions from each
623 combustion phase (pyrolysis, flaming and smouldering). Further investigation is needed in order to develop a better
624 understanding of these differences and to characterize the different combustion phases.

625 VOCs of intermediate volatility are suspected to be efficient precursors of SOA (Seinfeld and Pandis, 2006 and
626 references therein). However, as it was discussed in the section 3.4.3, our method was not able to resolve the
627 differences between VOC families and most SOA was assigned to aromatic compounds (up to 98%). Figure 10b
628 reports the fractional contribution and total emissions of IVOCs. Charcoal making, wood fuel burning, heavy-duty
629 diesel vehicles, and two-wheel vehicles represent the primary sources of these compounds, accounting for 58, 15, 12
630 and 11% of the total, respectively. Despite their lower emissions compared with aromatics or terpenes, IVOCs are
631 estimated to account for 80 Gg year⁻¹ of emissions in Côte d'Ivoire. A recent study observed that fine particles in
632 Abidjan are three times higher than the World Health Organization recommended concentrations (Djossou et al.,
633 2018). Hence, a better understanding of the aerosol precursors and formation processes is essential for the later
634 reduction of their concentrations in the urban atmosphere.

635 Oxygenated compounds were previously indicated as essential species in the emissions from burning sources
636 (Gilman et al., 2015; Hatch et al., 2015; Koss et al., 2018; Wiedinmyer et al., 2014). In addition, oxygenated
637 compounds like non-aromatics were dominant in the burning emission sources including a range of functional groups,
638 of which alcohols and carbonyls were the most abundant (Koss et al., 2018; Stockwell et al., 2015). Figure 10c
639 shows that aldehyde emissions are mainly governed by charcoal making, two-wheel vehicle and wood burning
640 sources (Figure 10c). In our study the quantified aldehydes represent only 5.5% of the total emissions of the country
641 (170 Gg year⁻¹). However, they can be essential compounds concerning reactivity and ozone formation. Hence,
642 further analysis of oxygenated compounds together with furans and other nitro-oxygenated compounds needs to be
643 addressed in future campaigns, in order to improve not only the quantification of these compounds but also provide
644 a better identification of the African tracers from biomass burning processes.

645

646 4. Summary and conclusions

647 This study reports for the first time a chemically detailed range of VOCs including C₅-C₁₆ alkanes, monoterpenes,
648 alkenes, aromatics and carbonyls compounds by using sorbent tubes during an intensive field campaign in Abidjan,
649 southern West Africa. We present here an original dataset integrating main emission sources and ambient
650 measurements from nine representative sites, and covering the urban spatial distribution of VOCs in Abidjan. The
651 spatial distribution and composition of VOC in ambient air in Abidjan reveals the effect of local burning and traffic
652 emissions. The highest concentrations were observed near domestic fires, landfill waste fires and traffic sites, in
653 agreement with the results reported in previous studies, when gas-phase and aerosols pollutants were measured.

654 The calculation of emission ratios is an important metric to evaluate the estimates provided by global emission
655 inventories. Emission ratios from regional-specific emission sources were established here and later used for the
656 analysis of fractional molar mass contribution and the estimation of potential VOC OH reactivity, ozone and

657 secondary organic aerosol formation. The distribution of VOC emissions (magnitude and composition) was different
658 for each evaluated source. Two wheel and heavy-duty vehicle sources presented the most significant total molar mass
659 emissions, while charcoal burning was the lowest. The sources related to burning processes, such as waste and wood
660 burning, also presented significant contribution to VOCs emissions. These sources represent common activities
661 present in Abidjan and might contribute a large quantity of VOC emissions to the southern West Africa region.

662 Regarding VOC speciation, molar mass contributions were mostly dominated by aromatic and alkane compounds.
663 Since few alkene species were quantified, aromatics ruled both ozone and SOA formation potential. However, the
664 SOA metrics applied here were not able to accurately analyse the other important SOA precursors contribution, such
665 as monoterpenes. Nevertheless, monoterpenes can contribute significantly to VOC OH reactivity from some sources
666 like waste burning, and the alkane species can significantly contribute to the total reactivity.

667 In order to estimate the magnitude of VOC emissions in Côte d'Ivoire, emission factors were determined from the
668 *in-situ* VOC database. Road transportation and residential profiles were obtained and compared with those reported
669 in global emission inventories (MACCcity and EDGAR). Our results revealed a discrepancy of up to a factor of 43
670 and 160 for residential and transport profiles when compared with both referenced inventories. The high levels of
671 VOC emissions obtained for Côte d'Ivoire outpace European emissions by up to a factor of 6. Interestingly,
672 monoterpene emissions were observed in anthropogenic emission sources from biomass burning to road
673 transportation sources, contributing to up to 340 Gg year⁻¹. These compounds are generally missing in the global
674 anthropogenic emission profiles, which would underestimate their impacts on air quality. This underestimation is not
675 only expected for Côte d'Ivoire but for all West Africa countries.

676 This study, in the framework of the DACCIWA project, allowed us for the first time to identify and quantify several
677 VOCs in ambient air and at emission sources in Abidjan, Côte d'Ivoire. Our results provide significant constraints
678 for the development of more realistic regional emission inventories. A continuous effort is needed to collect new
679 emission data and ambient measurements in West African countries for all critical atmospheric pollutants.

680

681 **Acknowledgments**

682 This work has received funding from the European Union Seventh Framework Programme (FP7/2007-2013) under
683 grant agreement number 603502 (EU project DACCIWA: Dynamics-aerosol-chemistry-cloud interactions in West
684 Africa). P Dominutti acknowledges the Postdoctoral Fellowship support from the Université Clermont Auvergne and
685 thanks the grant received from the CAPES program (Process N°: 88887.098995/2015-00, CAPES – PVE's Program,
686 2014) from the Ministry of Education of Brazil, during 2015-2016. Thierry Leonardis is thanked for the contribution
687 in the analysis of VOC sorbent tubes, graciously performed at the SAGE Department at IMT Lille Douai (France).

688

689 *Data availability.*

690 All data used in this study is available on the AERIS Data and Service Center, which can be found at
691 <http://baobab.sedoo.fr/DACCIWA>.

692

693 *Competing interests.* The authors declare that they have no conflict of interest.

694

696 **References**

- 697 AIRPARIF: Surveillance de la qualité de l'air en Ile-de-France., [online] Available from: <http://www.airparif.asso.fr/>
698 (Accessed 1 March 2018), 2016.
- 699 Ait-Helal, W., Borbon, A., Sauvage, S., de Gouw, J. A., Colomb, A., Gros, V., Freutel, F., Crippa, M., Afif, C.,
700 Baltensperger, U., Beekmann, M., Doussin, J.-F., Durand-Jolibois, R., Fronval, I., Grand, N., Leonardi, T., Lopez, M.,
701 Michoud, V., Miet, K., Perrier, S., Prévôt, A. S. H., Schneider, J., Siour, G., Zapf, P. and Locoge, N.: Volatile and
702 intermediate volatility organic compounds in suburban Paris: variability, origin and importance for SOA formation, *Atmos.*
703 *Chem. Phys.*, 14(19), 10439–10464, doi:10.5194/acp-14-10439-2014, 2014.
- 704 Akagi, S. K., Yokelson, R. J., Wiedinmyer, C., Alvarado, M. J., Reid, J. S., Karl, T., Crounse, J. D. and Wennberg, P. O.:
705 Emission factors for open and domestic biomass burning for use in atmospheric models, *Atmos. Chem. Phys.*, 11(9), 4039–
706 4072, doi:10.5194/acp-11-4039-2011, 2011.
- 707 Assamoi, E.-M. and Liousse, C.: A new inventory for two-wheel vehicle emissions in West Africa for 2002, *Atmos.*
708 *Environ.*, 44(32), 3985–3996, doi:10.1016/j.atmosenv.2010.06.048, 2010.
- 709 Atkinson, R. and Arey, J.: Atmospheric Degradation of Volatile Organic Compounds, *Chem. Rev.*, 103(12), 4605–4638,
710 doi:10.1021/cr0206420, 2003.
- 711 Bahino, J., Yoboué, V., Galy-Lacaux, C., Adon, M., Akpo, A., Keita, S., Liousse, C., Gardrat, E., Chiron, C., Ossouhou, M.,
712 Gnamien, S. and Djossou, J.: A pilot study of gaseous pollutants' measurement (NO₂, SO₂, NH₃, HNO₃ and O₃) in
713 Abidjan, Côte d'Ivoire: contribution to an overview of gaseous pollution in African cities, *Atmos. Chem. Phys.*, 18(7),
714 5173–5198, doi:10.5194/acp-18-5173-2018, 2018.
- 715 Baker, A. K., Beyersdorf, A. J., Doezema, L. a., Katzenstein, A., Meinardi, S., Simpson, I. J., Blake, D. R. and Sherwood,
716 F. R.: Measurements of nonmethane hydrocarbons in 28 United States cities, *Atmos. Environ.*, 42(1), 170–182,
717 doi:10.1016/j.atmosenv.2007.09.007, 2008.
- 718 Barletta, B., Meinardi, S., Simpson, I. J., Khwaja, H. a, Blake, D. R. and Rowland, F. S.: Mixing ratios of volatile organic
719 compounds (VOCs) in the atmosphere of Karachi, Pakistan, *Atmos. Environ.*, 36(21), 3429–3443, doi:10.1016/S1352-
720 2310(02)00302-3, 2002.
- 721 Bechara, J., Borbon, A., Jambert, C., Colomb, A. and Perros, P. E.: Evidence of the impact of deep convection on reactive
722 Volatile Organic Compounds in the upper tropical troposphere during the AMMA experiment in West Africa, *Atmos.*
723 *Chem. Phys.*, 10(21), 10321–10334, doi:10.5194/acp-10-10321-2010, 2010.
- 724 Bon, D., Ulbrich, I. and de Gouw, J. A.: Measurements of volatile organic compounds at a suburban ground site (T1) in
725 Mexico City during the MILAGRO 2006 campaign: measurement comparison, emission, *Atmos. Chem. Phys.*, 2011.
- 726 Borbon, A., Fontaine, H., Veillerot, M., Locoge, N., Galloo, J. C. and Guillermo, R.: An investigation into the traffic-
727 related fraction of isoprene at an urban location, *Atmos. Environ.*, 35(22), 3749–3760, doi:10.1016/S1352-2310(01)00170-
728 4, 2001.
- 729 Borbon, A., Locoge, N., Veillerot, M., GALLOO, J. C. and GUILLERMO, R.: Characterisation of NMHCs in a French
730 urban atmosphere: overview of the main sources, *Sci. Total Environ.*, 292(3), 177–191, doi:10.1016/S0048-
731 9697(01)01106-8, 2002.
- 732 Borbon, A., Gilman, J. B., Kuster, W. C., Grand, N., Chevallier, S., Colomb, A., Dolgorouky, C., Gros, V., Lopez, M.,
733 Sarda-Esteve, R., Holloway, J., Stutz, J., Petetin, H., McKeen, S., Beekmann, M., Warneke, C., Parrish, D. D. and de

734 Gouw, J. A.: Emission ratios of anthropogenic volatile organic compounds in northern mid-latitude megacities:
735 Observations versus emission inventories in Los Angeles and Paris, *J. Geophys. Res. Atmos.*, 118(4), 2041–2057,
736 doi:10.1002/jgrd.50059, 2013.

737 Borbon, A., Boynard, A., Salameh, T., Baudic, A., Gros, V., Gauduin, J., Perrussel, O. and Pallares, C.: Is Traffic Still an
738 Important Emitter of Monoaromatic Organic Compounds in European Urban Areas?, *Environ. Sci. Technol.*, 52(2), 513–
739 521, doi:10.1021/acs.est.7b01408, 2018.

740 Boynard, A., Borbon, A., Leonardis, T., Barletta, B., Meinardi, S., Blake, D. R. and Locoge, N.: Spatial and seasonal
741 variability of measured anthropogenic non-methane hydrocarbons in urban atmospheres: Implication on emission ratios,
742 *Atmos. Environ.*, 82, 258–267, doi:10.1016/j.atmosenv.2013.09.039, 2014.

743 Bracho-Nunez, A., Knothe, N. M., Welter, S., Staudt, M., Costa, W. R., Liberato, M. A. R., Piedade, M. T. F. and
744 Kesselmeier, J.: Leaf level emissions of volatile organic compounds (VOC) from some Amazonian and Mediterranean
745 plants, *Biogeosciences*, 10(9), 5855–5873, doi:10.5194/bg-10-5855-2013, 2013.

746 Brito, J., Wurm, F., Yáñez-Serrano, A. M., de Assunção, J. V., Godoy, J. M. and Artaxo, P.: Vehicular Emission Ratios of
747 VOCs in a Megacity Impacted by Extensive Ethanol Use: Results of Ambient Measurements in São Paulo, Brazil, *Environ.*
748 *Sci. Technol.*, 49(19), 11381–11387, doi:10.1021/acs.est.5b03281, 2015.

749 Brocco, D., Fratarcangeli, R., Lepore, L., Petricca, M. and Ventrone, I.: Determination of aromatic hydrocarbons in urban
750 air of Rome, *Atmos. Environ.*, 31(4), 557–566, doi:10.1016/S1352-2310(96)00226-9, 1997.

751 Deroubaix, A., Menut, L., Flamant, C., Brito, J., Denjean, C., Dreiling, V., Fink, A., Jambert, C., Kalthoff, N., Knippertz,
752 P., Ladkin, R., Mailler, S., Maranan, M., Pacifico, F., Piguet, B., Siour, G. and Turquety, S.: Diurnal cycle of coastal
753 anthropogenic pollutant transport over southern West Africa during the DACCIWA campaign, *Atmos. Chem. Phys.*, 19(1),
754 473–497, doi:10.5194/acp-19-473-2019, 2019.

755 Derwent, R. G., Jenkin, M. E., Saunders, S. M. and Pilling, M. J.: Photochemical ozone creation potentials for organic
756 compounds in northwest Europe calculated with a master chemical mechanism, *Atmos. Environ.*, 32(14–15), 2429–2441,
757 doi:10.1016/S1352-2310(98)00053-3, 1998.

758 Derwent, R. G., Jenkin, M. E., Passant, N. R. and Pilling, M. J.: Photochemical ozone creation potentials (POCPs) for
759 different emission sources of organic compounds, *Atmos. Environ.*, 41(12), 2570–2579,
760 doi:10.1016/j.atmosenv.2006.11.019, 2007.

761 Derwent, R. G., Jenkin, M. E., Utembe, S. R., Shallcross, D. E., Murrells, T. P. and Passant, N. R.: Secondary organic
762 aerosol formation from a large number of reactive man-made organic compounds, *Sci. Total Environ.*, 408(16), 3374–
763 3381, doi:10.1016/j.scitotenv.2010.04.013, 2010.

764 Detournay, A., Sauvage, S., Locoge, N., Gaudion, V., Leonardis, T., Fronval, I., Kaluzny, P. and Galloo, J.-C.:
765 Development of a sampling method for the simultaneous monitoring of straight-chain alkanes, straight-chain saturated
766 carbonyl compounds and monoterpenes in remote areas., *J. Environ. Monit.*, 13(4), 983–90, doi:10.1039/c0em00354a,
767 2011.

768 Djossou, J., Léon, J.-F., Akpo, A. B., Liousse, C., Yoboué, V., Bedou, M., Bodjrenou, M., Chiron, C., Galy-Lacaux, C.,
769 Gardrat, E., Abbey, M., Keita, S., Bahino, J., N'Datchoh, E. T., Ossohou, M. and Awanou, C. N.: Mass concentration,
770 optical depth and carbon composition of particulate matter in the major southern West African cities of Cotonou (Benin)
771 and Abidjan (Côte d'Ivoire), *Atmos. Chem. Phys.*, 18(9), 6275–6291, doi:10.5194/acp-18-6275-2018, 2018.

772 Dominutti, P. A., Nogueira, T., Borbon, A., Andrade, M. de F. and Fornaro, A.: One-year of NMHCs hourly observations

773 in São Paulo megacity: meteorological and traffic emissions effects in a large ethanol burning context, *Atmos. Environ.*,
774 142, 371–382, doi:10.1016/j.atmosenv.2016.08.008, 2016.

775 Epstein, S. A., Riipinen, I. and Donahue, N. M.: A Semiempirical Correlation between Enthalpy of Vaporization and
776 Saturation Concentration for Organic Aerosol, *Environ. Sci. Technol.*, 44(2), 743–748, doi:10.1021/es902497z, 2010.

777 Gaimoz, C., Sauvage, S., Gros, V., Herrmann, F., Williams, J., Locoge, N., Perrussel, O., Bonsang, B., D'Argouges, O.,
778 Sarda-Estève, R. and Sciare, J.: Volatile organic compounds sources in Paris in spring 2007. Part II: source apportionment
779 using positive matrix factorisation, *Environ. Chem.*, 8(1), 91, doi:10.1071/EN10067, 2011.

780 Gilman, J. B., Lerner, B. M., Kuster, W. C., Goldan, P. D., Warneke, C., Veres, P. R., Roberts, J. M., De Gouw, J. A.,
781 Burling, I. R. and Yokelson, R. J.: Biomass burning emissions and potential air quality impacts of volatile organic
782 compounds and other trace gases from fuels common in the US, *Atmos. Chem. Phys.*, 15(24), 13915–13938,
783 doi:10.5194/acp-15-13915-2015, 2015.

784 de Gouw, J. A., Gilman, J. B., Kim, S.-W., Lerner, B. M., Isaacman-VanWertz, G., McDonald, B. C., Warneke, C., Kuster,
785 W. C., Lefer, B. L., Griffith, S. M., Dusanter, S., Stevens, P. S. and Stutz, J.: Chemistry of Volatile Organic Compounds in
786 the Los Angeles basin: Nighttime Removal of Alkenes and Determination of Emission Ratios, *J. Geophys. Res. Atmos.*,
787 122(21), 11,843–11,861, doi:10.1002/2017JD027459, 2017.

788 Granier, C., Bessagnet, B., Bond, T., D'Angiola, A., Denier van der Gon, H., Frost, G. J., Heil, A., Kaiser, J. W., Kinne, S.,
789 Klimont, Z., Kloster, S., Lamarque, J.-F., Liousse, C., Masui, T., Meleux, F., Mieville, A., Ohara, T., Raut, J.-C., Riahi, K.,
790 Schultz, M. G., Smith, S. J., Thompson, A., van Aardenne, J., van der Werf, G. R. and van Vuuren, D. P.: Evolution of
791 anthropogenic and biomass burning emissions of air pollutants at global and regional scales during the 1980–2010 period,
792 *Clim. Change*, 109(1–2), 163–190, doi:10.1007/s10584-011-0154-1, 2011.

793 Hatch, L. E., Luo, W., Pankow, J. F., Yokelson, R. J., Stockwell, C. E. and Barsanti, K. C.: Identification and quantification
794 of gaseous organic compounds emitted from biomass burning using two-dimensional gas chromatography-time-of-flight
795 mass spectrometry, *Atmos. Chem. Phys.*, 15(4), 1865–1899, doi:10.5194/acp-15-1865-2015, 2015.

796 Heeb, N. V., Forss, A.-M., Bach, C., Reimann, S., Herzog, A. and Jäckle, H. W.: A comparison of benzene, toluene and
797 C2-benzenes mixing ratios in automotive exhaust and in the suburban atmosphere during the introduction of catalytic
798 converter technology to the Swiss Car Fleet, *Atmos. Environ.*, 34(19), 3103–3116, doi:10.1016/S1352-2310(99)00446-X,
799 2000.

800 Huang, G., Brook, R., Crippa, M., Janssens-Maenhout, G., Schieberle, C., Dore, C., Guizzardi, D., Muntean, M., Schaaf, E.
801 and Friedrich, R.: Speciation of anthropogenic emissions of non-methane volatile organic compounds: A global gridded
802 data set for 1970–2012, *Atmos. Chem. Phys.*, 17(12), 7683–7701, doi:10.5194/acp-17-7683-2017, 2017.

803 Jaars, K., Beukes, J. P., Van Zyl, P. G., Venter, A. D., Josipovic, M., Pienaar, J. J., Vakkari, V., Aaltonen, H., Laakso, H.,
804 Kulmala, M., Tiitta, P., Guenther, A., Hellén, H., Laakso, L. and Hakola, H.: Ambient aromatic hydrocarbon measurements
805 at Welgegund, South Africa, *Atmos. Chem. Phys.*, 14(13), 7075–7089, doi:10.5194/acp-14-7075-2014, 2014.

806 Jaars, K., Van Zyl, P. G., Beukes, J. P., Hellén, H., Vakkari, V., Josipovic, M., Venter, A. D., Räsänen, M., Knoetze, L.,
807 Cilliers, D. P., Siebert, S. J., Kulmala, M., Rinne, J., Guenther, A., Laakso, L. and Hakola, H.: Measurements of biogenic
808 volatile organic compounds at a grazed savannah grassland agricultural landscape in South Africa, *Atmos. Chem. Phys.*,
809 16(24), 15665–15688, doi:10.5194/acp-16-15665-2016, 2016.

810 Jenkin, M. E., Derwent, R. G. and Wallington, T. J.: Photochemical ozone creation potentials for volatile organic
811 compounds: Rationalization and estimation, *Atmos. Environ.*, 163(x), 128–137, doi:10.1016/j.atmosenv.2017.05.024, 2017.

812 Keita, S., Liousse, C., Yoboué, V., Dominutti, P., Guinot, B., Assamoi, E.-M., Borbon, A., Haslett, S. L., Bouvier, L.,
813 Colomb, A., Coe, H., Akpo, A., Adon, J., Bahino, J., Doumbia, M., Djossou, J., Galy-Lacaux, C., Gardrat, E., Gnamien, S.,
814 Léon, J. F., Ossohou, M., N'Datchoh, E. T. and Roblou, L.: Particle and VOC emission factor measurements for
815 anthropogenic sources in West Africa, *Atmos. Chem. Phys.*, 18(10), 7691–7708, doi:10.5194/acp-18-7691-2018, 2018.

816 Knippertz, P., Coe, H., Chiu, J. C., Evans, M. J., Fink, A. H., Kalthoff, N., Liousse, C., Mari, C., Allan, R. P., Brooks, B.,
817 Danour, S., Flamant, C., Jegede, O. O., Lohou, F. and Marsham, J. H.: The DACCIWA Project: Dynamics–Aerosol–
818 Chemistry–Cloud Interactions in West Africa, *Bull. Am. Meteorol. Soc.*, 96(9), 1451–1460, doi:10.1175/BAMS-D-14-
819 00108.1, 2015a.

820 Knippertz, P., Evans, M. J., Field, P. R., Fink, A. H., Liousse, C. and Marsham, J. H.: The possible role of local air
821 pollution in climate change in West Africa, *Nat. Clim. Chang.*, 5(9), 815–822, doi:10.1038/nclimate2727, 2015b.

822 Knippertz, P., Fink, A. H., Deroubaix, A., Morris, E., Tocquer, F., Evans, M. J., Flamant, C., Gaetani, M., Lavaysse, C.,
823 Mari, C., Marsham, J. H., Meynadier, R., Affo-Dogo, A., Bahaga, T., Brosse, F., Deetz, K., Guebsi, R., Latifou, I.,
824 Maranan, M., Rosenberg, P. D. and Schlueter, A.: A meteorological and chemical overview of the DACCIWA field
825 campaign in West Africa in June–July 2016, *Atmos. Chem. Phys.*, 17(17), 10893–10918, doi:10.5194/acp-17-10893-2017,
826 2017.

827 Koss, A. R., Sekimoto, K., Gilman, J. B., Selimovic, V., Coggon, M. M., Zarzana, K. J., Yuan, B., Lerner, B. M., Brown,
828 S. S., Jimenez, J. L., Krechmer, J., Roberts, J. M., Warneke, C., Yokelson, R. J. and De Gouw, J.: Non-methane organic gas
829 emissions from biomass burning: Identification, quantification, and emission factors from PTR-ToF during the FIREX
830 2016 laboratory experiment, *Atmos. Chem. Phys.*, 18(5), 3299–3319, doi:10.5194/acp-18-3299-2018, 2018.

831 Kumar, A., Singh, D., Kumar, K., Singh, B. B. and Jain, V. K.: Distribution of VOCs in urban and rural atmospheres of
832 subtropical India: Temporal variation, source attribution, ratios, OFP and risk assessment, *Sci. Total Environ.*, 613–614,
833 492–501, doi:10.1016/j.scitotenv.2017.09.096, 2018.

834 Liousse, C., Assamoi, E., Criqui, P., Granier, C. and Rosset, R.: Explosive growth in African combustion emissions from
835 2005 to 2030, *Environ. Res. Lett.*, 9(3), 035003, doi:10.1088/1748-9326/9/3/035003, 2014.

836 Manion, J. A., Huie, R. E., Levin, R. D., Jr., D. R. B., Orkin, V. L., Tsang, W., McGivern, W. S., Hudgens, J. W., Knyazev,
837 V. D., Atkinson, D. B., Chai, E., Tereza, A. M., Lin, C.-Y., Allison, T. C., Mallard, W. G., Westley, F., Herron, J. T., R. F.
838 Hampson, A. and Frizzell, D. H.: NIST Chemical Kinetics Database, Gaithersburg, Maryland. [online] Available from:
839 <http://kinetics.nist.gov/> (Accessed 18 April 2018), 2015.

840 Mari, C. H., Reeves, C. E., Law, K. S., Ancellet, G., Andrés-Hernández, M. D., Barret, B., Bechara, J., Borbon, A.,
841 Bouarar, I., Cairo, F., Commane, R., Delon, C., Evans, M. J., Fierli, F., Floquet, C., Galy-Lacaux, C., Heard, D. E., Homan,
842 C. D., Ingham, T., Larsen, N., Lewis, A. C., Liousse, C., Murphy, J. G., Orlandi, E., Oram, D. E., Saunois, M., Serça, D.,
843 Stewart, D. J., Stone, D., Thouret, V., Velthoven, P. van and Williams, J. E.: Atmospheric composition of West Africa:
844 Highlights from the AMMA international program, *Atmos. Sci. Lett.*, 12(1), 13–18, doi:10.1002/asl.289, 2011.

845 Muezzinoglu, A., Odabasi, M. and Onat, L.: Volatile organic compounds in the air of Izmir, Turkey, *Atmos. Environ.*,
846 35(4), 753–760, doi:10.1016/S1352-2310(00)00420-9, 2001.

847 Niedojadlo, A., Becker, K. H., Kurtenbach, R. and Wiesen, P.: The contribution of traffic and solvent use to the total
848 NMVOC emission in a German city derived from measurements and CMB modelling, *Atmos. Environ.*, 41(33), 7108–
849 7126, doi:10.1016/j.atmosenv.2007.04.056, 2007.

850 OpenStreetMap contributors: Maps of Abidjan area, Available from: www.openstreetmap.org (Accessed 20 August 2019),

851 2015.

852 Robinson, A. L., Donahue, N. M., Shrivastava, M. K., Weitkamp, E. a, Sage, A. M., Grieshop, A. P., Lane, T. E., Pierce, J.
853 R. and Pandis, S. N.: Rethinking Organic Aerosols: Semivolatile Emissions and Photochemical Aging, *Science* (80-.),
854 315(5816), 1259–1262, doi:10.1126/science.1133061, 2007.

855 Salameh, T., Afif, C., Sauvage, S., Borbon, A. and Locoge, N.: Speciation of non-methane hydrocarbons (NMHCs) from
856 anthropogenic sources in Beirut, Lebanon, *Environ. Sci. Pollut. Res.*, 21(18), 10867–10877, doi:10.1007/s11356-014-2978-
857 5, 2014.

858 Salameh, T., Sauvage, S., Afif, C., Borbon, A., Léonardis, T., Brioude, J., Waked, A. and Locoge, N.: Exploring the
859 seasonal NMHC distribution in an urban area of the Middle East during ECOCEM campaigns: Very high loadings
860 dominated by local emissions and dynamics, *Environ. Chem.*, 12(3), 316–328, doi:10.1071/EN14154, 2015.

861 Salameh, T., Borbon, A., Afif, C., Sauvage, S., Leonardis, T., Gaimoz, C. and Locoge, N.: Composition of gaseous organic
862 carbon during ECOCEM in Beirut, Lebanon: new observational constraints for VOC anthropogenic emission evaluation in
863 the Middle East, *Atmos. Chem. Phys. Discuss.*, (August), 1–32, doi:10.5194/acp-2016-543, 2016a.

864 Salameh, T., Sauvage, S., Afif, C., Borbon, A. and Locoge, N.: Source apportionment vs. emission inventories of non-
865 methane hydrocarbons (NMHC) in an urban area of the Middle East: local and global perspectives, *Atmos. Chem. Phys.*,
866 16(5), 3595–3607, doi:10.5194/acp-16-3595-2016, 2016b.

867 Saxton, J. E., Lewis, A. C., Kettlewell, J. H., Ozel, M. Z., Gogus, F., Boni, Y., Korogone, S. O. U. and Serça, D.: Isoprene
868 and monoterpene emissions from secondary forest in northern Benin, *Atmos. Chem. Phys. Discuss.*, 7(2), 4981–5012,
869 doi:10.5194/acpd-7-4981-2007, 2007.

870 von Schneidmesser, E., Monks, P. S. and Plass-Duelmer, C.: Global comparison of VOC and CO observations in urban
871 areas, *Atmos. Environ.*, 44(39), 5053–5064, doi:10.1016/j.atmosenv.2010.09.010, 2010.

872 von Schneidmesser, E., Monks, P. S., Gros, V., Gauduin, J. and Sanchez, O.: How important is biogenic isoprene in an
873 urban environment? A study in London and Paris, *Geophys. Res. Lett.*, 38(19), doi:10.1029/2011GL048647, 2011.

874 Seinfeld, J. H. and Pandis, S. N.: *Atmospheric Chemistry and Physics. From Air Pollution to Climate Change*, Second edi.,
875 John Wiley & Sons., 2006.

876 Sekimoto, K., Koss, A. R., Gilman, J. B., Selimovic, V., Coggon, M. M., Zarzana, K. J., Yuan, B., Lerner, B. M., Brown,
877 S. S., Warneke, C., Yokelson, R. J., Roberts, J. M. and de Gouw, J.: High- and low-temperature pyrolysis profiles describe
878 volatile organic compound emissions from western US wildfire fuels, *Atmos. Chem. Phys.*, 18(13), 9263–9281,
879 doi:10.5194/acp-18-9263-2018, 2018.

880 SIE CI: Rapport Côte d’Ivoire Energie 2010., , 57 [online] Available from:
881 http://www.ecowrex.org/system/files/repository/2010_rapport_annuel_sie_-_min_ener.pdf (Accessed 27 August 2018),
882 2010.

883 Simpson, I. J., Akagi, S. K., Barletta, B., Blake, N. J., Choi, Y., Diskin, G. S., Fried, A., Fuelberg, H. E., Meinardi, S.,
884 Rowland, F. S., Vay, S. A., Weinheimer, A. J., Wennberg, P. O., Wiebring, P., Wisthaler, A., Yang, M., Yokelson, R. J.
885 and Blake, D. R.: Boreal forest fire emissions in fresh Canadian smoke plumes: C1-C10 volatile organic compounds
886 (VOCs), CO₂, CO, NO₂, NO, HCN and CH₃CN, *Atmos. Chem. Phys.*, 11(13), 6445–6463, doi:10.5194/acp-11-6445-
887 2011, 2011.

888 Sommariva, R., De Gouw, J. A., Trainer, M., Atlas, E., Goldan, P. D., Kuster, W. C., Warneke, C. and Fehsenfeld, F. C.:
889 Emissions and photochemistry of oxygenated VOCs in urban plumes in the Northeastern United States, *Atmos. Chem.*

890 Phys., 11(14), 7081–7096, doi:10.5194/acp-11-7081-2011, 2011.

891 Sommers, W. T., Loehman, R. A. and Hardy, C. C.: Wildland fire emissions, carbon, and climate: Science overview and
892 knowledge needs, *For. Ecol. Manage.*, 317, 1–8, doi:10.1016/j.foreco.2013.12.014, 2014.

893 Stockwell, C. E., Veres, P. R., Williams, J. and Yokelson, R. J.: Characterization of biomass burning emissions from
894 cooking fires, peat, crop residue, and other fuels with high-resolution proton-transfer-reaction time-of-flight mass
895 spectrometry, *Atmos. Chem. Phys.*, 15(2), 845–865, doi:10.5194/acp-15-845-2015, 2015.

896 United Nations: World Population Prospects: The 2017 Revision, Dep. Econ. Soc. Aff. - Popul. Div., 2017.

897 Wang, M., Shao, M., Chen, W., Yuan, B., Lu, S., Zhang, Q., Zeng, L. and Wang, Q.: A temporally and spatially resolved
898 validation of emission inventories by measurements of ambient volatile organic compounds in Beijing, China, *Atmos.*
899 *Chem. Phys.*, 14(12), 5871–5891, doi:10.5194/acp-14-5871-2014, 2014.

900 Wang, Y.-F., Owen, S. M., Li, Q.-J. and Peñuelas, J.: Monoterpene emissions from rubber trees (*Hevea brasiliensis*) in a
901 changing landscape and climate: chemical speciation and environmental control, *Glob. Chang. Biol.*, 13(11), 2270–2282,
902 doi:10.1111/j.1365-2486.2007.01441.x, 2007.

903 Warneke, C., McKeen, S. a., de Gouw, J. a., Goldan, P. D., Kuster, W. C., Holloway, J. S., Williams, E. J., Lerner, B. M.,
904 Parrish, D. D., Trainer, M., Fehsenfeld, F. C., Kato, S., Atlas, E. L., Baker, a. and Blake, D. R.: Determination of urban
905 volatile organic compound emission ratios and comparison with an emissions database, *J. Geophys. Res.*, 112(D10),
906 D10S47, doi:10.1029/2006JD007930, 2007.

907 Wiedinmyer, C., Yokelson, R. J. and Gullett, B. K.: Global Emissions of Trace Gases, Particulate Matter, and Hazardous
908 Air Pollutants from Open Burning of Domestic Waste, *Environ. Sci. Technol.*, 48(16), 9523–9530, doi:10.1021/es502250z,
909 2014.

910 Yokelson, R. J., Burling, I. R., Gilman, J. B., Warneke, C., Stockwell, C. E., De Gouw, J., Akagi, S. K., Urbanski, S. P.,
911 Veres, P., Roberts, J. M., Kuster, W. C., Reardon, J., Griffith, D. W. T., Johnson, T. J., Hosseini, S., Miller, J. W., Cocker,
912 D. R., Jung, H. and Weise, D. R.: Coupling field and laboratory measurements to estimate the emission factors of identified
913 and unidentified trace gases for prescribed fires, *Atmos. Chem. Phys.*, 13(1), 89–116, doi:10.5194/acp-13-89-2013, 2013.

914 Zhang, Q., Yuan, B., Shao, M., Wang, X., Lu, S., Lu, K., Wang, M., Chen, L., Chang, C.-C. and Liu, S. C.: Variations of
915 ground-level O₃ and its precursors in Beijing in summertime between 2005 and 2011, *Atmos. Chem. Phys.*, 14(12), 6089–
916 6101, doi:10.5194/acp-14-6089-2014, 2014.

917

918

919 List of figures

920 **Figure 1.** Geographical location of Abidjan, Côte d'Ivoire and spatial distribution of ambient VOC measurements. Red stars
921 indicate the VOC measurement sites and the blue square represents the meteorology site. More information about the ambient
922 site is detailed in Table 2. Map: ©OpenStreetMap contributors (OpenStreetMap contributors, 2015)

923 **Figure 2.** Meteorological data observed in Abidjan, Côte d'Ivoire. The figure represents a) the weekly accumulated
924 precipitation (in mm month⁻¹) and weekly mean air temperature (in °C) and b) the wind speed (in m s⁻¹) and direction observed
925 (deg), during the field campaigns (2016). Data was downloaded from the National Centers for environmental information
926 site (NCDC), NOAA and recorded at Abidjan International Airport (see location in Figure 1).

927 **Figure 3.** Spatial distribution of VOCs measured at ambient sites in Abidjan, size-coded by the sum of VOCs (in µg m⁻³) and
928 color-coded by the relative contribution of BTEX compounds (% in mass), namely m+p-xylene (m+p-xyl), toluene (Tol), o-
929 xylene (o-xyl), ethylbenzene (EthylB), benzene (Benz), and other VOC. Values shown in each pie-chart represent the total
930 VOC concentration measured at the sampling point. Ambient site names and characteristics are presented in Table 2. Map:
931 ©OpenStreetMap contributors (OpenStreetMap contributors, 2015)

932 **Figure 4.** Boxplot showing the VOC concentrations (µg m⁻³) at Abidjan ambient sites (upper panel). The middle line in each
933 box plot indicates the median (50th percentile), the lower and upper box limits represent the 25th and 75th quartiles,
934 respectively, and the whiskers the 99% coverage assuming the data has a normal distribution. The lower panel shows the
935 mean concentrations reported in other cities worldwide, such as Abidjan - Côte d'Ivoire (this study), Paris - France
936 (AIRPARIF, 2016), São Paulo - Brazil (Dominutti et al., 2016), Beirut - Lebanon (Salameh et al., 2014), Karachi - Pakistan
937 (Barletta et al., 2002) and Welgegund - South Africa (Jaars et al., 2014).

938 **Figure 5.** Relative concentration comparison between ambient measurements and emission source profiles of VOCs
939 measured in Abidjan, Côte d'Ivoire. Orange and yellow based colours represent the contributions of alkanes, blue based
940 colours aromatics, and green-based colours terpenes and isoprene.

941 **Figure 6.** Contribution of VOC reported in Table S1 to the measured molar mass of anthropogenic sources analysed in
942 Abidjan, aggregated in VOC families (Table S2). The emission sources under analysis are heavy-duty diesel vehicles
943 (HDDV), two-wheel two-stroke vehicles (TW2T), two-wheel four-stroke vehicles (TW4T), light-duty diesel vehicles
944 (LDDV), light-duty gasoline vehicles (LDGV), charcoal burning (CH), wood fuel burning (FW), charcoal making (CHM)
945 and waste burning (WB). Values in the upper panel represent the total measured molar mass (in µg cm⁻³ ppm CO⁻¹) of the
946 respective anthropogenic source.

947 **Figure 7.** Contributions of VOC emission ratios to (a)–(d) the measured molar mass, (e)–(h) OH reactivity, (i)–(l) relative
948 ozone formation potential POCP and (m)–(p) relative SOA formation potential, aggregated in VOC families. Absolute totals
949 for each source are shown below each pie chart in the respective units.

950 **Figure 8.** Comparison of VOC emission profiles for Côte d'Ivoire from the emissions estimated from the measurements of
951 this study and the EDGAR v4.3.2 (Huang et al., 2017) and MACCcity inventories (Granier et al., 2011). The profile analysis
952 integrates road transportation and residential sectors based on the sector activity for 2012. a) absolute emissions, in Tg year⁻¹,
953 b) relative mass contribution, and c) relative mass reactivity, considering 100 Tg of emissions weighted by the k_{OH} reaction
954 rate calculated for each VOC family.

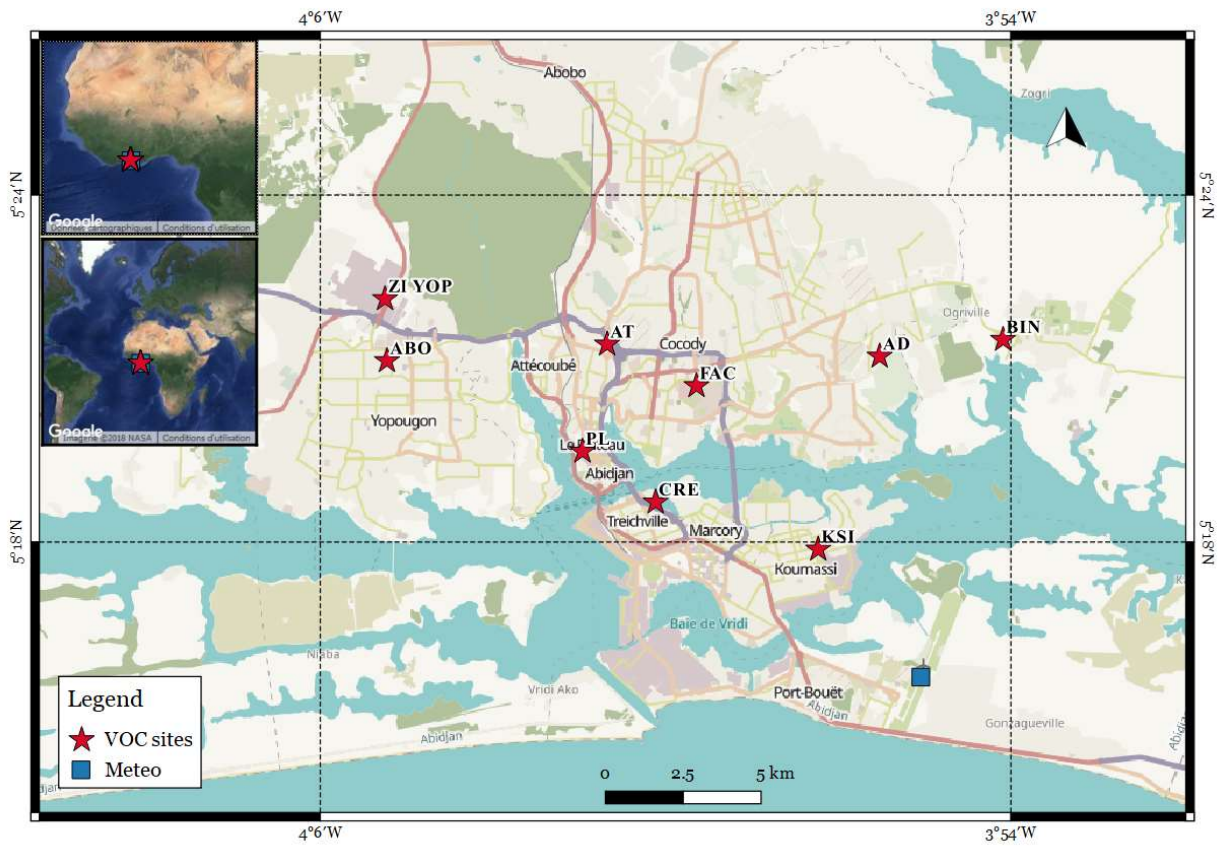
955 **Figure 9.** VOC emission profiles considering all the VOC families calculated from the measurements of our study and
956 compared with the global EDGAR v4.3.2 inventory (Huang et al., 2017). The comparison integrates road transportation (RT)
957 and residential (Resid) sectors in Côte d'Ivoire and Europe for the year 2012. Absolute emissions are expressed in Gg year⁻¹
958 for each VOC group.

959 **Figure 10.** Total estimated emissions and relative distributions in the anthropogenic sources measured in Côte d'Ivoire for
960 the VOC family a) Terpenes, b) IVOCs and c) Aldehydes (* for aldehydes species >C₆).

961 **Figure 11.** Distribution of monoterpenes and isoprene in the emission sources measured in Abidjan. The values represent the
962 percentage of each terpenoids over the total emission estimated for these species.

963

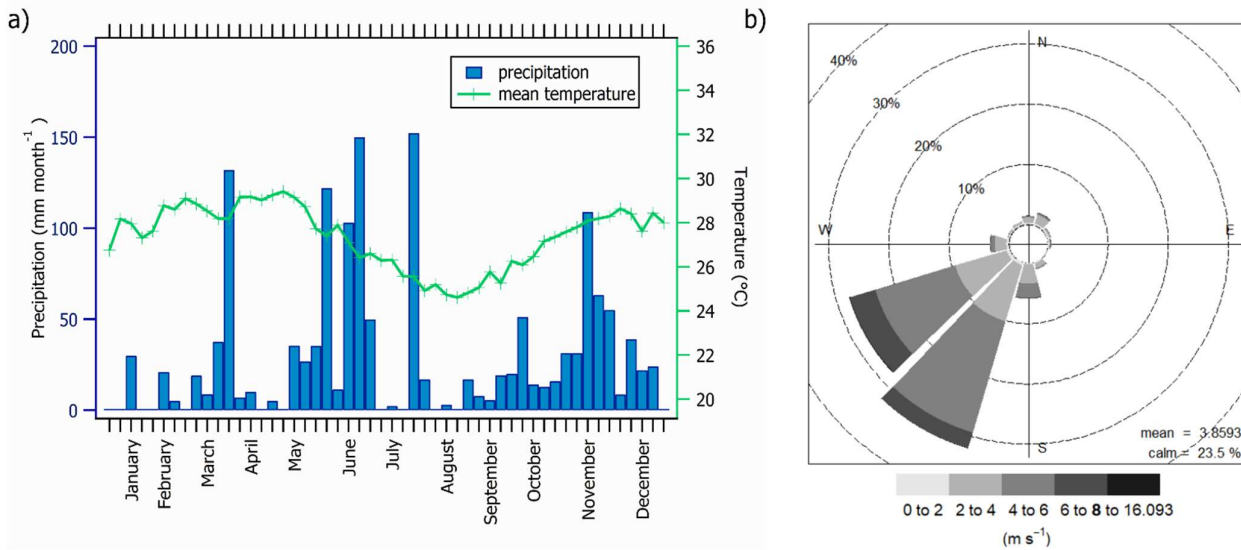
964



965

966 **Figure 1.** Geographical location of Abidjan, Côte d'Ivoire and spatial distribution of ambient VOC measurements.
 967 Red stars indicate the VOC measurement sites and the blue square represents the meteorology site. More
 968 information about the ambient site is detailed in Table 2. Map: ©OpenStreetMap contributors (OpenStreetMap
 969 contributors, 2015)

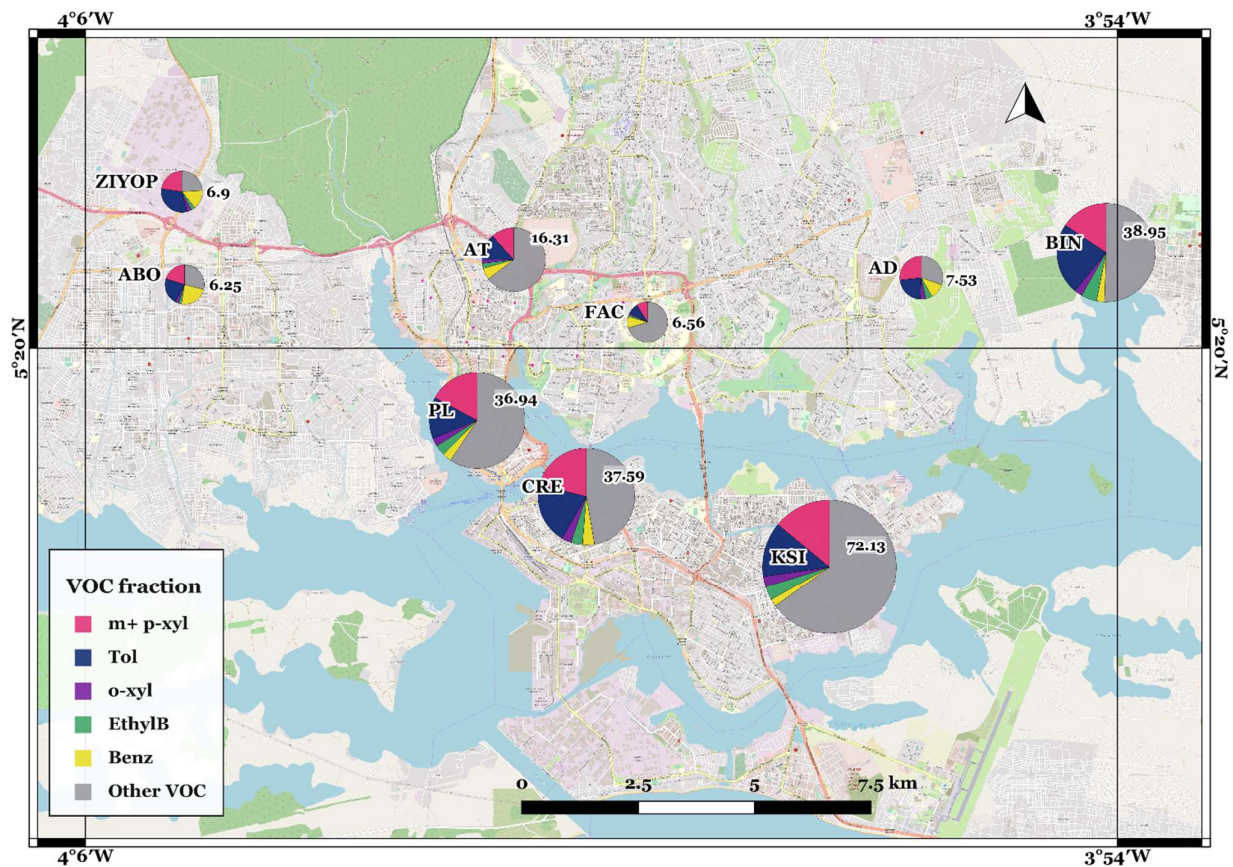
970



971

972 **Figure 2.** Meteorological data observed in Abidjan, Côte d'Ivoire. The figure represents a) the weekly
 973 accumulated precipitation (in mm month⁻¹) and weekly mean air temperature (in °C) and b) the wind speed (in m
 974 s⁻¹) and direction observed (deg), during the field campaigns (2016). Data was downloaded from the National
 975 Centers for environmental information site (NCDC), NOAA and recorded at Abidjan International Airport (see
 976 location in Figure 1).

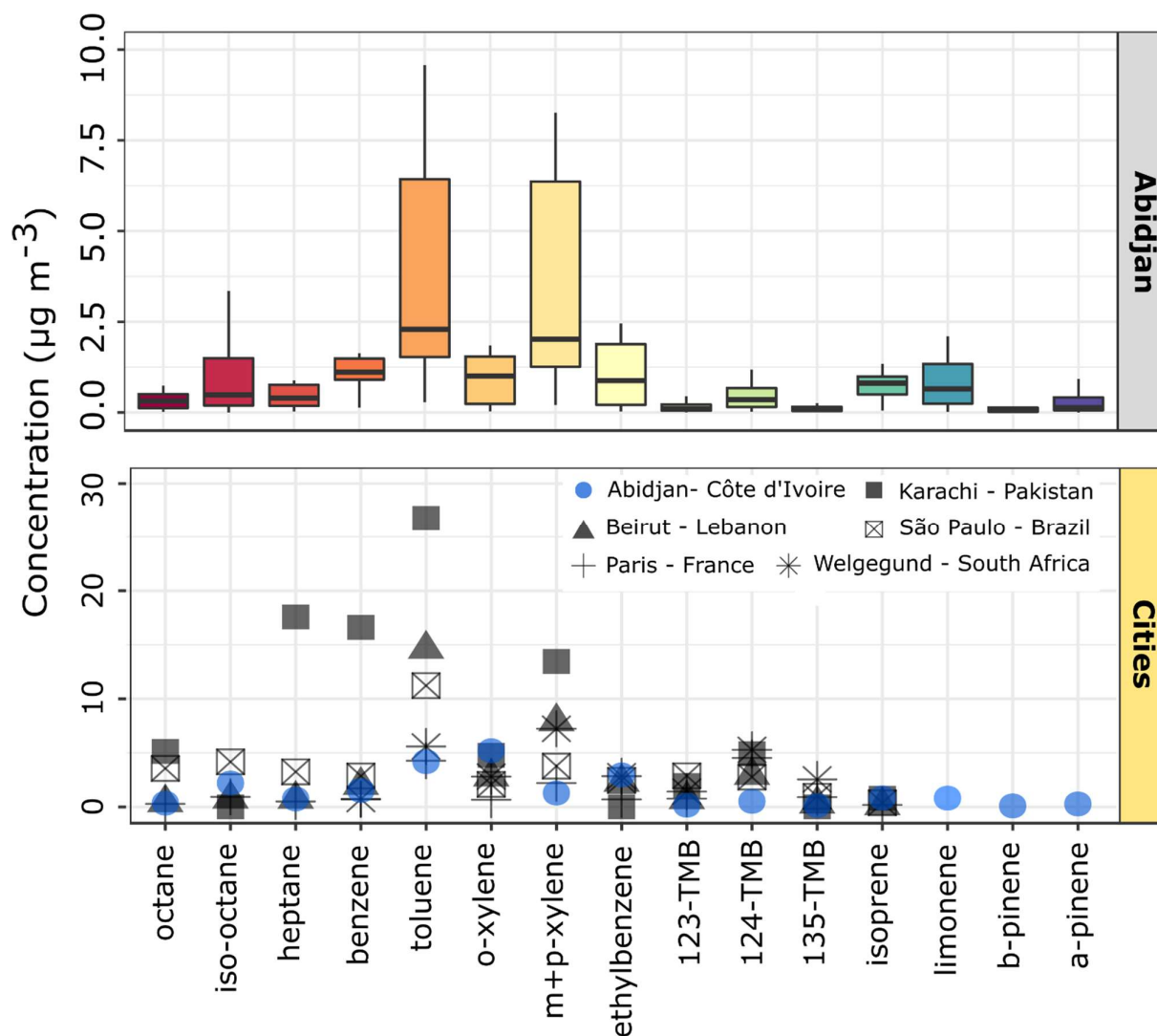
977



978
 979 **Figure 3.** Spatial distribution of VOCs measured at ambient sites in Abidjan, size-coded by the sum of VOCs (in
 980 $\mu\text{g m}^{-3}$) and color-coded by the relative contribution of BTEX compounds (% in mass), namely m+p-xylene (m+p-
 981 xyl), toluene (Tol), o-xylene (o-xyl), ethylbenzene (EthylB), benzene (Benz), and other VOC. Values shown in
 982 each pie-chart represent the total VOC concentration measured at the sampling point. Ambient site names and
 983 characteristics are presented in Table 2. Map: ©OpenStreetMap contributors (OpenStreetMap contributors, 2015)

984

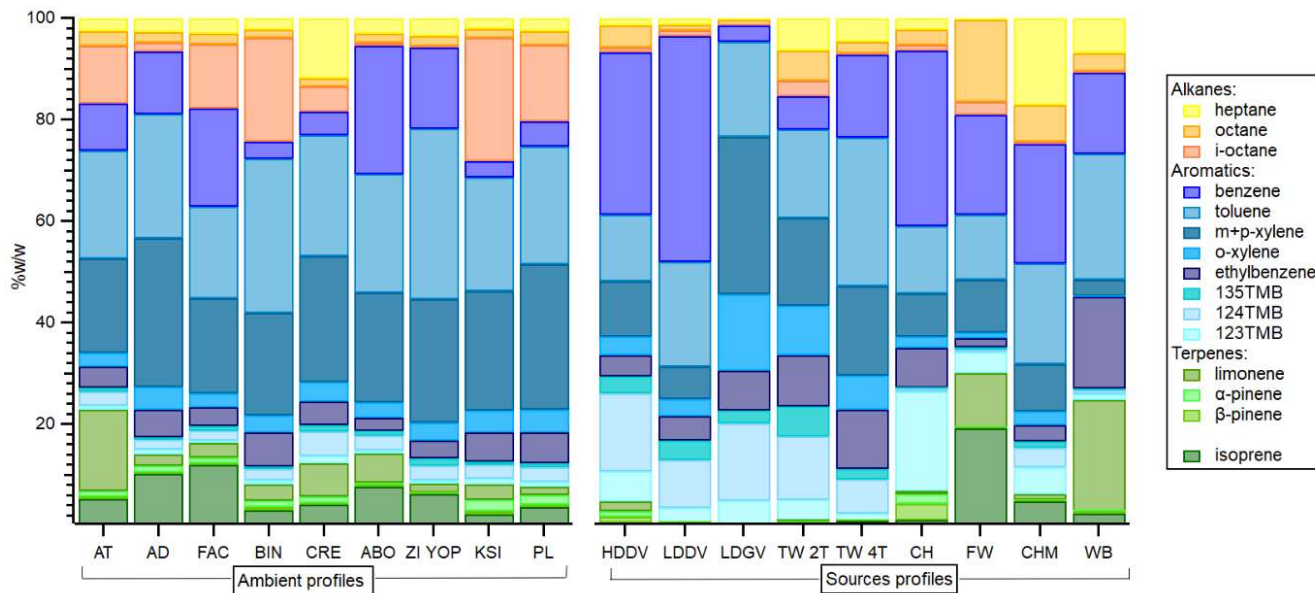
985



986
987

988 **Figure 4.** Boxplot showing the VOC concentrations ($\mu\text{g m}^{-3}$) at Abidjan ambient sites (upper panel). The middle
989 line in each box plot indicates the median (50th percentile), the lower and upper box limits represent the 25th and
990 75th quartiles, respectively, and the whiskers the 99% coverage assuming the data has a normal distribution. The
991 lower panel shows the mean concentrations reported in other cities worldwide, such as Abidjan - Côte d'Ivoire
992 (this study), Paris - France (AIRPARIF, 2016), São Paulo - Brazil (Dominutti et al., 2016), Beirut - Lebanon
993 (Salameh et al., 2014), Karachi - Pakistan (Barletta et al., 2002) and Welgegund - South Africa (Jaars et al., 2014).

994



996

997 **Figure 5.** Relative concentration comparison between ambient measurements and emission source profiles of
 998 VOCs measured in Abidjan, Côte d'Ivoire. Orange and yellow based colours represent the contributions of
 999 alkanes, blue based colours aromatics, and green-based colours terpenes and isoprene.

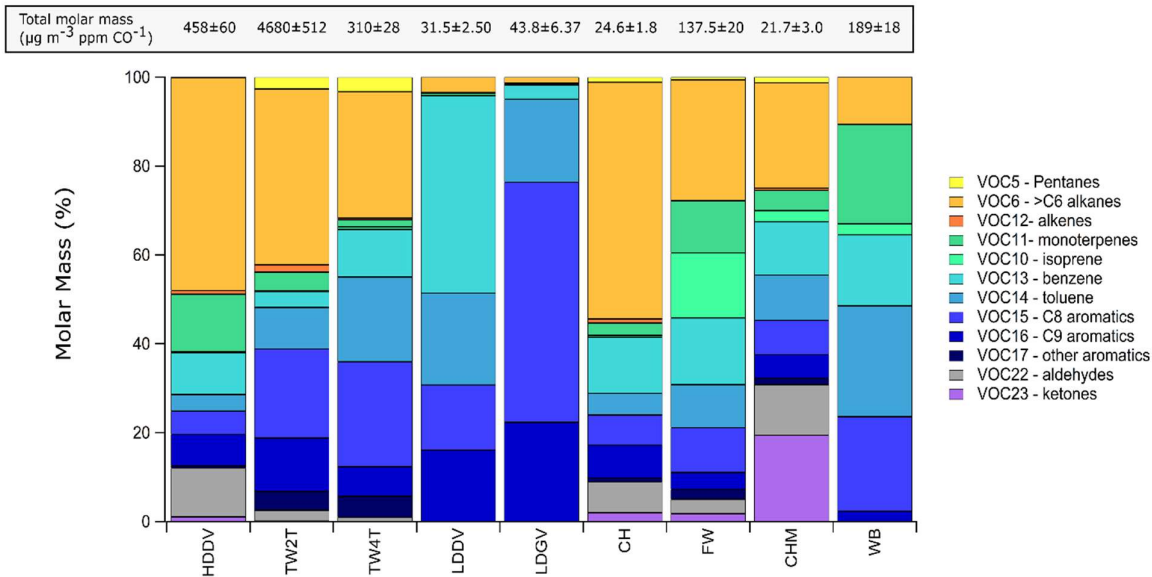
1000

1001

1002

1003

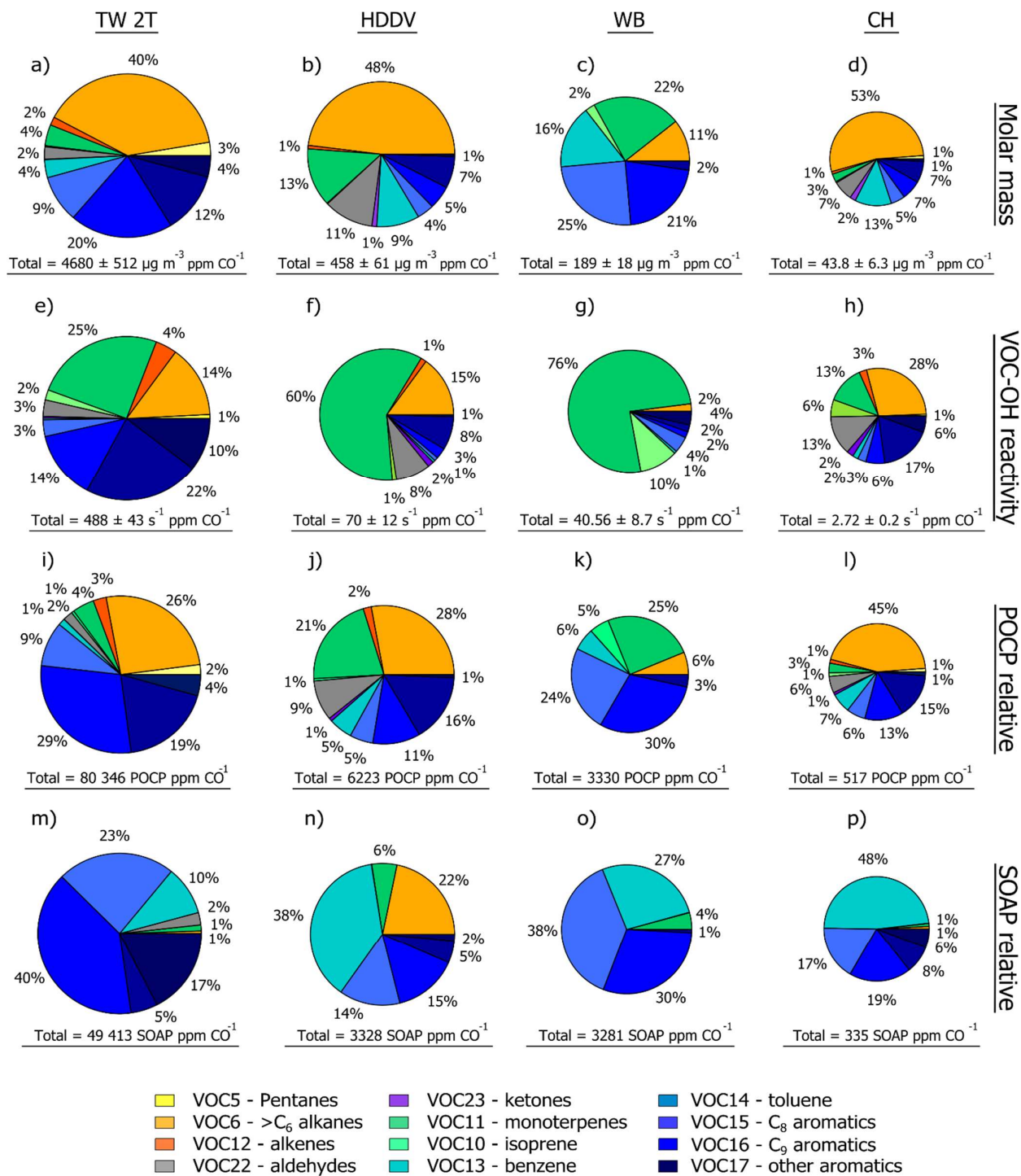
1004



1005

1006 **Figure 6.** Contribution of VOC reported in Table S1 to the measured molar mass of anthropogenic sources
1007 analysed in Abidjan, aggregated in VOC families (Table S2). The emission sources under analysis are heavy-duty
1008 diesel vehicles (HDDV), two-wheel two-stroke vehicles (TW2T), two-wheel four-stroke vehicles (TW4T), light-
1009 duty diesel vehicles (LDDV), light-duty gasoline vehicles (LDGV), charcoal burning (CH), wood fuel burning
1010 (FW), charcoal making (CHM) and waste burning (WB). Values in the upper panel represent the total measured
1011 molar mass (in $\mu\text{g cm}^{-3}$ ppm CO^{-1}) of the respective anthropogenic source.

1012



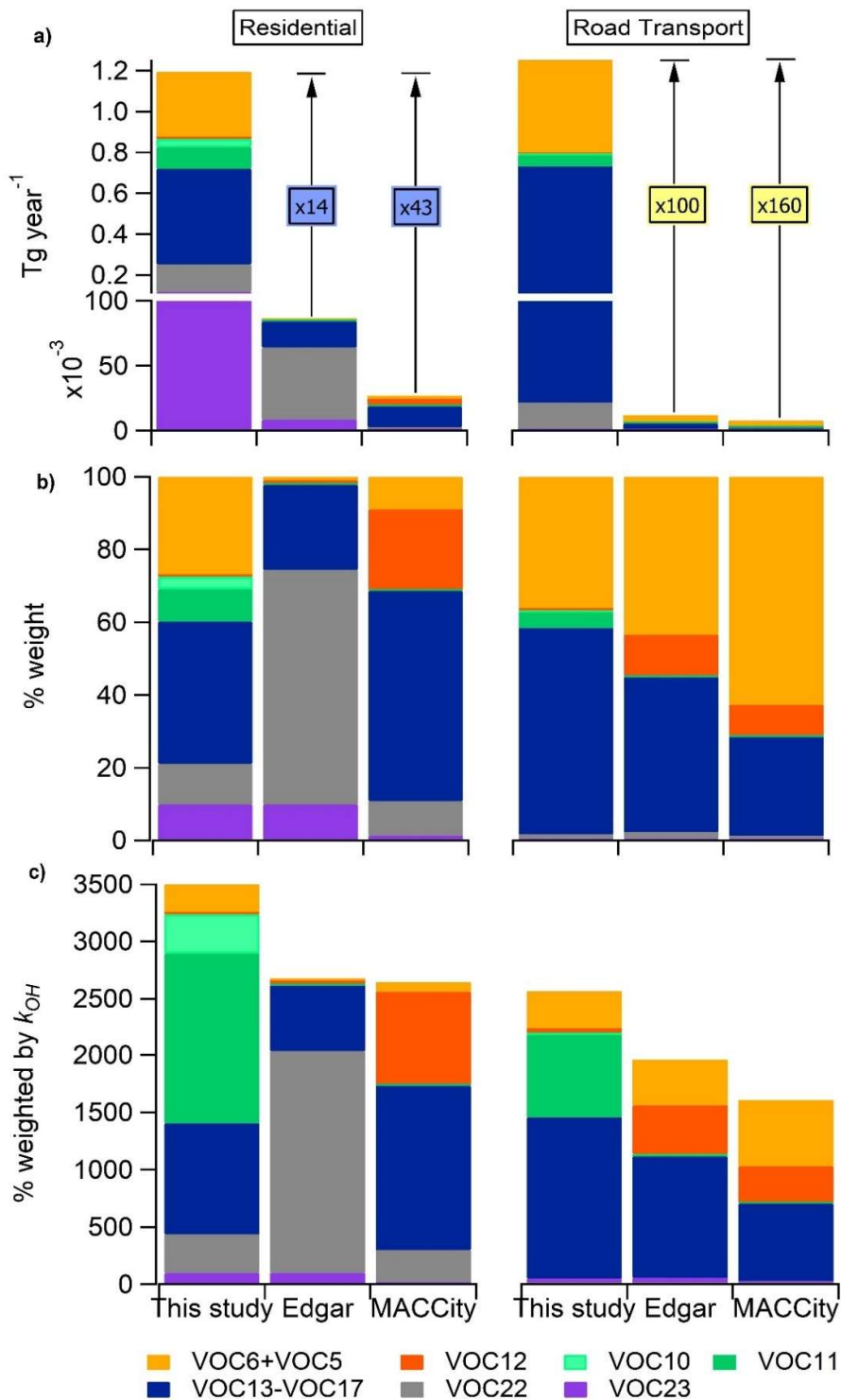
1015

1016

1017 **Figure 7.** Contributions of VOC emission ratios to (a)–(d) the measured molar mass, (e)–(h) OH reactivity, (i)–
 1018 (l) relative ozone formation potential POCP and (m)–(p) relative SOA formation potential, aggregated in VOC
 1019 families. Absolute totals for each source are shown below each pie chart in the respective units.

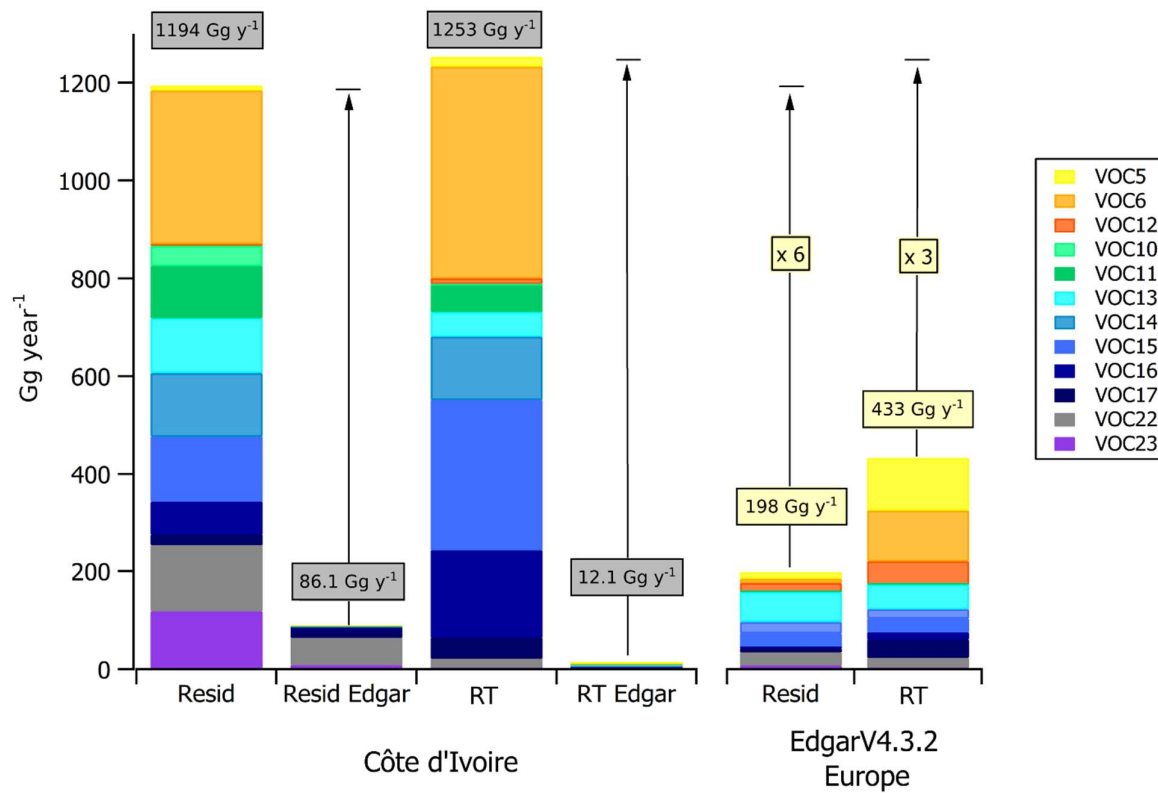
1020

1021



1022

1023 **Figure 8.** Comparison of VOC emission profiles for Côte d'Ivoire from the emissions estimated from the
 1024 measurements of this study and the EDGAR v4.3.2 (Huang et al., 2017) and MACCity inventories (Granier et al.,
 1025 2011). The profile analysis integrates road transportation and residential sectors based on the sector activity for
 1026 2012. a) absolute emissions, in Tg year⁻¹, b) relative mass contribution, and c) relative mass reactivity, considering
 1027 100 Tg of emissions weighted by the k_{OH} reaction rate calculated for each VOC family.



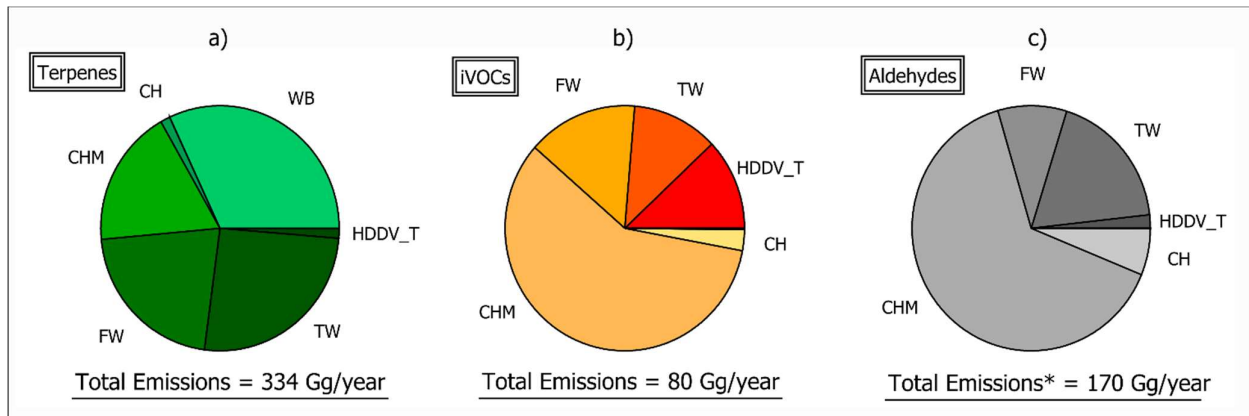
1029

1030 **Figure 9.** VOC emission profiles considering all the VOC families calculated from the measurements of our study
 1031 and compared with the global EDGAR v4.3.2 inventory (Huang et al., 2017). The comparison integrates road
 1032 transportation (RT) and residential (Resid) sectors in Côte d'Ivoire and Europe for the year 2012. Absolute
 1033 emissions are expressed in Gg year⁻¹ for each VOC group.

1034

1035

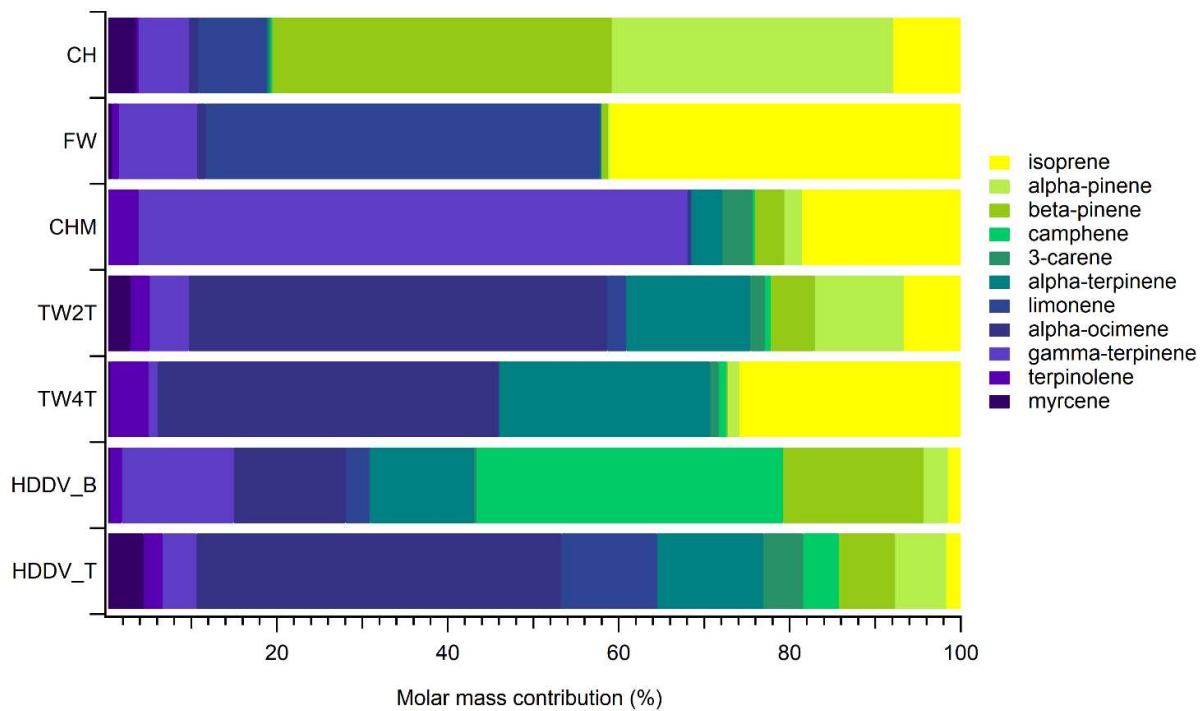
1036



1037

1038 **Figure 10.** Total estimated emissions and relative distributions in the anthropogenic sources measured in Côte
1039 d'Ivoire for the VOC family a) Terpenes, b) iVOCs and c) Aldehydes (* for aldehydes species >C₆).

1040



1041

1042 **Figure 11.** Distribution of monoterpenes and isoprene in the emission sources measured in Abidjan. The values
 1043 represent the percentage of each terpenoids over the total emission estimated for these species.

1044

1045

1046
1047
1048
1049
1050
1051
1052
1053

List of Tables

- Table 1. Description of the emission sources measured and evaluated in Abidjan, Côte d'Ivoire.
Table 2. Geographical location and characteristics of ambient measurement sites in Abidjan, Côte d'Ivoire

Table 1. Description of the emission sources measured and evaluated in Abidjan, Côte d'Ivoire.

| Reference | Sub-group | Description | source | type |
|-----------|-----------|------------------------------|--|----------------|
| HDDV | | Heavy-duty diesel vehicles | Diesel emissions | Road Transport |
| | HDDV-T | Diesel trucks | Diesel emissions | Road Transport |
| | HDDV-B | Diesel buses | Diesel emissions | Road Transport |
| LDDV | | Light-duty diesel vehicles | Diesel emissions | Road Transport |
| LDGV | | Light-duty gasoline vehicles | Gasoline emissions | Road Transport |
| TW | TW2T | Two-wheel two-stroke | a mixture of smuggled oil and gasoline | Road Transport |
| | TW4T | Two-wheel four-stroke | a mixture of smuggled oil and gasoline | Road Transport |
| CH | | Charcoal | Charcoal burning | Residential |
| FW | | Wood fuel burning | <i>Hevea brasiliensis</i> | Residential |
| CHM | | Charcoal making | Charcoal fabrication | Residential |
| WB | | Waste burning | Domestic landfill burning | Waste burning |

Table 2. Geographical location and characteristics of ambient measurement sites in Abidjan, Côte d'Ivoire

| ID | Site location | Longitude | Latitude | Activity |
|--------|---------------|------------|------------|--|
| AT | Adjame | 04°01'04"W | 05°21'14"N | Traffic site. Site near a gbaka public transport station; regular traffic jams; obsolete public transport vehicles (gbaka, shared taxis and buses); human activities |
| AD | Akouédo | 03°56'16"W | 05°21'12"N | Landfill waste burning Uncontrolled landfill, continuous waste burning of all types of waste |
| FAC | Cocody | 03°59'27"W | 05°20'42"N | Residential. University residences; electric vehicles; new personal vehicles; use of liquefied petroleum gas (LPG) for cooking |
| BIN | Bingerville | 03°54'07"W | 05°21'30"N | Urban Background Far from traffic, near to Ebrié Lagoon |
| CRE | Treichville | 04°00'10"W | 05°18'41"N | Green urban area, Near to Ebrié Lagoon; windy |
| ABO | Abobo | 04°04'10"W | 05°26'08"N | Traffic + residential Townhall, near to the big market of Abobo. Old communal taxis and minibuses in a crowded crossroad, human activities |
| ZI YOP | Yopougon | 04°04'52"W | 05°22'12"N | Industrial area Heavy industries (cement plants) and light industries (agro-industries, plastic and iron processing, pharmaceutical and cosmetics industries); heavy goods vehicles, traffic jams |
| KSI | Koumassi | 03°57'20"W | 05°17'52"N | Domestic fires + traffic Residential site mainly influenced by domestic activities, fire-wood, and charcoal; old vehicles. |
| PL | Plateau | 04°01'26"W | 05°19'33"N | Traffic/administrative City center, crossroad with traffic jams; light-duty vehicles, near the train station |